
APPLICATION DEVELOPMENT OF LIGNIN IN VALUABLE ENGINEERING POLYMERS VIA MILD THERMOCHEMICAL AND MECHANOCHEMICAL PROCESS

Authors

ORGANIZATION

Jinwen Zhang



Washington State
University

Michael Wolcott



Washington State
University

Junna Xin



Washington State
University

Xiaojie Guo



Washington State
University

Xiaoxu Teng

Yangtze Normal University, China

Jianglei Qin

Hebei University, China

Mei Li

Institute of Chemical Industry of
Forestry Products, China

COMPLETED 2016

TABLE OF CONTENTS

LIST OF FIGURES.....	3
LIST OF TABLES.....	4
LIST OF ACRONYMS	4
EXECUTIVE SUMMARY.....	5
INTRODUCTION	6
TASK 1:	7
APPLICATION DEVELOPMENT OF LIGNIN-BASED EPOXIES USING PARTIALLY DEPOLYMERIZED LIGNIN	
TASK 2:	21
EXPLORE DEPOLYMERIZATION AND MODIFICATION OF LIGNIN IN SOLID STATE REACTION	
NARA OUTPUTS	29
NARA OUTCOMES	30
FUTURE DEVELOPMENT	30
LIST OF REFERENCES	31

nararenewables.org  **BY-NC-ND**



NARA is led by Washington State University and supported by the Agriculture and Food Research Initiative Competitive Grant no. 2011-68005-30416 from the USDA National Institute of Food and Agriculture.



Any opinions, findings, conclusions, or recommendations expressed in this publication are those of the author(s) and do not necessarily reflect the view of the U.S. Department of Agriculture.

LIST OF FIGURES

FIGURE NO.	FIGURE TITLE	PAGE NO.	FIGURE NO.	FIGURE TITLE	PAGE NO.
PL-1.1.	NMR spectra of Eu-EP and intermediates at different stages of the synthesis.....	08	PL-1.18.	Effects of epoxy resin contents on the rheological properties of modified asphalt blends by PDL-epoxy and DER332, respectively.	19
PL-1.2.	Dynamic mechanical properties of cured DER353/HHPA (squares), Eu-EP/HHPA (circles) and Eu-EP (triangles).....	08	PL-1.19.	Effects of epoxy resin contents on the rheological properties of modified asphalt blends by PDL-EA-MA/DER332 and PDL-MPA/DER33, respectively.....	20
PL-1.3.	Effect of NaOH concentration on yield.	09	PL-2.1.	¹ H-NMR spectra of model compound with (a) oleated products and (b) succinate product through solution reactions.....	21
PL-1.4.	Effects of temperature (a) and catalyst content (b) on yield of hydrogenation of lignin.....	10	PL-2.2.	¹ H-NMR spectra of model compound with succinate product through ball milling.....	22
PL-1.5.	³¹ P NMR spectra of before and after hydrogenation of lignin at different temperatures.....	11	PL-2.3.	FT-IR spectra of NARA lignin and oleated Lginin w/ and w/o milling medium.	23
PL-1.6.	Comparisons of solubility of lignins between before (a) and after hydrogenolysis (b).	11	PL-2.4.	Images of hot pressed samples for (a) NARA (wood milled) lignin and (b) LMO (no Na ₂ SO ₄) at 200 oC, and for (c) LMO (Na ₂ SO ₄) at 150 oC.LMO: lignin modified by methyl oleate.....	23
PL-1.7.	³¹ P NMR of PDL and LPCA (a) and FTIR spectra of lignin and derivatives (b).....	12	PL-2.5.	DMA curves of tan delta versus temperature of unmodified and oleated lignin.....	23
PL-1.8.	DSC curves of DER 353/LPCA with different ratios.....	13	PL-2.6.	Photos of (a) extrudate of PLA/lignin (70/30 w/w) blends through melt extrusion and (b) sample bars of PLA/lignin (70/30 w/w) blends through injection molding.....	24
PL-1.9.	Storage modulus (a) and tan δ versus temperature for DER353/LPCA with different ratio.....	13	PL-2.7.	SEM images of flat-cut surfaces for (a) PLA/NARA lignin blends, (b) PLA/LMO (non Na ₂ SO ₄) blends and (c) PLA/LMO (Na ₂ SO ₄) blends.	24
PL-1.10.	Storage modulus (a) and tan δ versus temperature for DER353 resin cured with LPCA/GTA.....	13	PL-2.8.	DSC curves of PLA/lignin blends: (a) first cooling and (b) second heating.....	24
PL-1.11.	Storage modulus (a) and tan δ versus temperature for DER353 resin cured with LPCA/HHPA.....	14	PL-2.9.	FT-IR spectra of unmodified and esterified nara lignins with: (a) succinic anhydride and (b) maleic anhydride.....	26
PL-1.12.	The FTIR spectra of PDL, PDL-epoxy-70 °C and PDL-epoxy-117 °C.....	16	PL-2.10.	DSC exotherms of curing processes of tricomponent resin systems at heating rates of 2.5, 5, 7.5, 10 and 12.5 °C/min.....	26
PL-1.13.	³¹ P NMR spectra of PDL and PDL epoxies.....	16	PL-2.11.	Plot of ln ϕ versus 1/Tpby Qzawa method.....	27
PL-1.14.	Comparisons of the non-isothermal curing of the PDL-epoxy and DER 332 at different heating rates (a, b) and the plots of 1/(Tp) versus (c, d).....	17	PL-2.12.	Storage modulus (a), loss modulus (b) and tan delta (c) of cured LPCA-NMA-DER353 versus temperature.....	27
PL-1.15.	Storage modulus and tan δ versus temperature for DER332 and PDL-epoxy cured with ME-MA.....	17	PL-2.13.	TGA curves of cured LPCA-NMA-DER353 resins.....	28
PL-1.16.	Comparison of thermal stability of cured PDL-epoxy and DER 332 resins.....	18			
PL-1.17.	The FTIR spectra of PDL, PDL-EA-MA and PDL-MPA.....	18			

LIST OF TABLES

TABLE NO.	TABLE TITLE
PL-1.1.	DSC results of non-isothermal curing and thermal stability of the cured eugenol epoxies07
PL-1.2.	Depolymerization of lignins by the BCD method09
PL-1.3.	Yield obtained from different reaction systems10
PL-1.4.	Characterization of the depolymerized lignins by GPC and 31P NMR11
PL-1.5.	Effect of co-curing agents on Tg and thermal stability of the cured epoxy resins14
PL-1.6.	Hydroxyl values of PDL and PDL-epoxies determined by 31P NMR16
PL-1.7.	DSC results of non-isothermal curing and thermal properties of cured epoxies.....17
PL-2.1.	Thermal properties of the PLA and lignin blends24
PL-2.2.	Mechanical properties of the PLA/lignin blends25
PL-2.3.	Activation energy (Ea) and glass transition temperature (Tg).....27

LIST OF ACRONYMS

PDL	Partial depolymerized lignin
PLA	Polylactic acid
KL	Kraft lignin
m-CPBA	meta-chloroperoxybenzoic acid
ECH	epichlorohydrin
Eu-Ep	the epoxy obtained from eugenol
HPHA	Hexahydrophthalic Anhydride
DMA	dynamic mechanical analysis
FTIR	fourier transform infrared spectroscopy
DA	Diluted acid
WO	Wet oxidation
CLE	Catchlight energy's sugar process
SEM	scanning electron microscopy
DMBA	N, N-dimthylbenzylamine
DER353	Commercial epoxy
LMO	Lignin modified by methyl oleate
PALMO	purifiedacetylated LMO
SANL	Lignin modified by succinic anhydride
TGA	thermogravimetric analysis
MPA	maleopimaric acid
BPA	Bisphenol A
DSC	differential scanning calorimetry
EMID	2-ethyl-4-methylimidazole
DCM	dichloromethane
1H NMR	proton nuclear magnetic resonance
13C NMR	carbon nuclear magnetic resonance
P NMR	Phosphorus nuclear magnetic resonance
LPCA	Lignin-based polycarboxylic acids
DMSO	dimethylsulfoxide
TLC	Thin layer chromatography
GPC	Gel permeation chromatograph
GTA	glyceroltris(succinate monoester)
NL	NARA lignin
ALMO	acetylated LMO
LPCA	Lignin based polycarboxylic acid
MANL	Lignin modified by maleic anhydride

EXECUTIVE SUMMARY

Lignin has received a lot of study for applications in both thermoplastic and thermosetting polymer materials. Lignin is characteristic of aromatic and branched molecular structure and has a lot of phenolic and alcoholic hydroxyl groups. Compatibility is a major issue for lignin use in polymer materials. In order to improve the compatibility of lignin with other ingredients in thermosetting polymer application, lignin was partially depolymerized via either hydrogenolysis or base-catalyzed approaches under mild conditions. The effects of various reaction parameters on yield of depolymerization were investigated. The partial depolymerized lignin (PDL) is a low molecular weight oligomer with increased hydroxyl value. PDL displayed greatly enhanced solubility in organic solvents and

was further used to synthesize lignin based epoxy monomers and polycarboxylic acid curing agents. Results showed that the epoxy resin based on from PDL-derived epoxy monomers or curing agent exhibited good mechanical and thermal properties. Lignin-based epoxy resin was also utilized to modify asphalt for higher performance. On the other hand, for the thermoplastic polymer application, a solvent free method, mechanochemical approach was employed to depolymerize and simultaneously modify lignin via transesterification with methyl oleate in a ball milling process. The oleated lignin was blended with PLA and the properties of the PLA/lignin blends could be greatly regulated by adjusting the composition of the blends.

INTRODUCTION

Using lignin for polymer materials has received extensive investigations from academia and industry. However, neither the direct use of lignin as polymeric component nor the use of depolymerized lignin as a monomeric feedstock for polymer materials have achieved significant progress to date [Hofmann & Classer, 1994; Sun et al., 2007]. Currently, commercially available lignin is mainly limited to the Kraft lignin (KL) and sulfonated lignin (lignosulfonate). KL and lignosulfonate are recovered from the spent pulping liquids of their respective pulping processes and are available in various product forms. While lignosulfonates are mainly used as industrial dispersants, KL has far fewer practical applications [Yang et al., 2007]. Nonetheless, in recent years KL has received tremendous interest in polymer applications [Li et al. 2012a; Li et al. 2012b. As our nation strives to advance the technology of lignocellulosic biorefinery, a huge amount of hydrolysis lignin is expected to be available.

Lignin-to-chemical conversion is a highly desirable approach in lignin utilization and could potentially produce many important aromatic chemicals including intermediate monomeric feedstock [Pandey & Kim, 2011; Yan et al., 2008]. Scientists are striving to explore various technologies to selectively cleave lignin for desirable chemicals. Meanwhile, plant scientists and biochemists also seek means to interrupt the normal biosynthesis of lignin and harvest the precursor chemicals directly. While these efforts may eventually result in significant progress and advance the related sciences, they are not likely to achieve breakthrough technologies any time soon.

As seen in the growing number of scientific publications, the presence of both phenolic and alcohol hydroxyls makes lignin an attractive substance to directly incorporate into existing thermosetting resins as a reactive ingredient or extender [Cateto et al., 2009; Chen et al., 2012;]. *However, compatibility remains the major*

issue in these applications. Similar compatibility issues are also present when lignin is used as volume filler for thermoplastic polymers. The poor compatibility between lignin and other systems is rooted in its highly branched molecular structure, which makes it neither miscible with nor accessible to others for good interactions. In addition, lignin as a base material for thermoplastics is another important application but still faces many processing problems [Li & Sarkanen, 2002; Li & Sarkanen, 2005].

Complete lignin depolymerization is an energy-negative process aimed at deconstructing what nature has constructed. Instead, *increasing the use of and adding value to the lignin polymer that nature has already provided is more attractive for the chemical industry.* **In this project, we developed new technologies for the preparation of engineering polymers from NARA lignin and to explore the applications.** The characteristic structure of lignin makes lignin insoluble in most organic solvents and hinders the access of hydroxyls for modification reactions. As indicated above, to completely disintegrate the lignin structure and use the resulting monomeric chemicals for construction of new polymers is not practical and may not be economically advantageous. In this project, partially depolymerized lignin (PDL) with enhanced solubility will provide accessible hydroxyls to enhance modification, thereby converting the lignin into effective building blocks for engineering polymers. Epoxy resin is the target polymer in this current effort but it will not be the only application interest long-term. Attention will be given to other engineering polymers when an appropriate application is identified. Furthermore, PDL is expected to possess an improved performance when directly incorporated as an active ingredient to thermosets because the reduced molecular weight and increased accessibility and content of hydroxyls promote compatibility and/or even the miscibility. The implementation of this project consists of three major tasks.

TASK 1: APPLICATION DEVELOPMENT OF LIGNIN-BASED EPOXIES USING PARTIALLY DEPOLYMERIZED LIGNIN

1.1. Preparation of epoxy monomer using eugenol

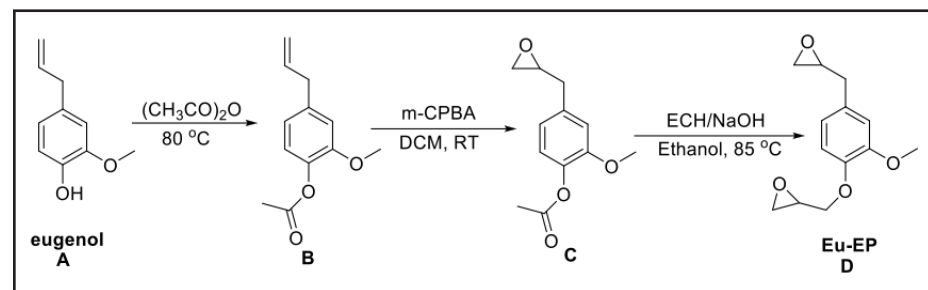
Objective

Eugenol is a valuable chemical and is used in perfume. Eugenol can be obtained from a number of plant extractives and is also claimed to be present in lignin cracking products by some researchers. If the lignin-to-chemical technology becomes viable, there will be a lot of eugenol available for other applications. Therefore, in this task, we demonstrated the synthesis of an epoxy using eugenol as feedstock. Scheme PL-1.1 shows the synthesis route and reaction conditions. A rosin-derived anhydride was also prepared and used as a biobased curing agent. The curing kinetics of the eugenol epoxy with the rosin-derived anhydride curing agent and with a commercial anhydride curing agent was studied using DSC. Dynamic mechanical properties and thermal stability of the cured resins were also studied using DMA and TGA, respectively. The major aims of this study were to provide a synthesis method for a eugenol-derived epoxy and to compare its properties with that of the BPA-type epoxies in applications.

Methodology

In Scheme PL-1.1, the hydroxyl group in eugenol was first protected by acetylation then the double bond was oxidized by *m*-CPBA followed by glycidylation using epichlorohydrin (ECH). This synthetic route was proved to be successful in preparing an epoxy monomer. The yield for each step was 93% for B, 91% for C and 63% for D, respectively.

The obtained epoxy (Eu-EP) from eugenol was cured with a commercial curing agent hexahydrophthalic anhydride (HHPA) and rosin based curing agent (maleopimaric acid, MPA) in an equivalent ratio of 1:0.8 and 1-ethyl-4-methylimidazole (EMID) as catalyst. The mixture were ground in a mortar at ~60 °C to obtain a homogeneous mixture. EMID was added at 0.1 eq with respect to HHPA and 0.15 eq with respect to MPA. The homogeneous mixture of Eu-EP, curing agents and EMID was transferred to a steel mold with five cavities of rectangular shape. The resins were cured first at 150 °C for 2 h and then at 200 °C for 4 h. The DMA and TGA specimens were prepared using these cured samples.



Scheme PL-1.1. Synthesis of epoxy from eugenol.

Results

Figure PL-1.1 shows the ^1H NMR spectra of the intermediates at different stages in the synthesis of Eu-EP. After acetylation, the peak at 5.51 ppm (j) attributed to the phenolic hydroxyls (Fig. PL-1.1(a)) disappeared completely, and a new peak at 2.30 ppm (n) attributed to the protons of acetyl groups confirmed the formation of acetyl eugenol (Fig. PL-1.1(b)). Furthermore, by comparing the peak areas of n and m, it is revealed that all hydroxyl groups in eugenol were acetylated. The oxidation of acetyl eugenol (B) with *m*-CPBA was performed at room temperature in DCM. It is noted that acetyl eugenol oxide (C) was the only product of this reaction. The yield of this reaction was ~91%. The ^1H NMR spectra show that the signals of the protons of the double bonds at 5.09 and 5.95 ppm (k in Fig. PL-1.1(b)) disappeared completely and new peaks attributed to oxiranes appeared at 2.54, 2.84 and 3.14 ppm (l, o and p in Fig. PL-1.1(c)). Although the product was not specially purified, the ^1H NMR spectrum suggests that the product is of high purity.

Table PL-1.1 summarizes the results of the non-isothermal curing. Without using catalyst, curing of Eu-EP/HHPA exhibited a broad exothermic peak with a peak temperature of $214.2\text{ }^\circ\text{C}$ and heat of reaction of 237 J g^{-1} . On the other hand, curing of Eu-EP/MPA exhibited a broader exothermic peak with a peak temperature of $230.4\text{ }^\circ\text{C}$ and a much lower heat of reaction of 69.9 J g^{-1} . Because MPA is a solid with high melting point, curing of Eu-EP/MPA without catalyst is probably far from completion as reflected in the very low heat of reaction. As a high-temperature curing agent, anhydride is often used with imidazole-type catalysts to reduce curing temperature. When 0.08 eq EMID was added to Eu-EP/HHPA, the curing temperature decreased drastically. Compared to the curing without catalyst, the overall heat of reaction (445 J g^{-1}) was almost doubled. This result suggests that curing without catalyst was only partially completed even at a temperature up to $300\text{ }^\circ\text{C}$. Similarly,

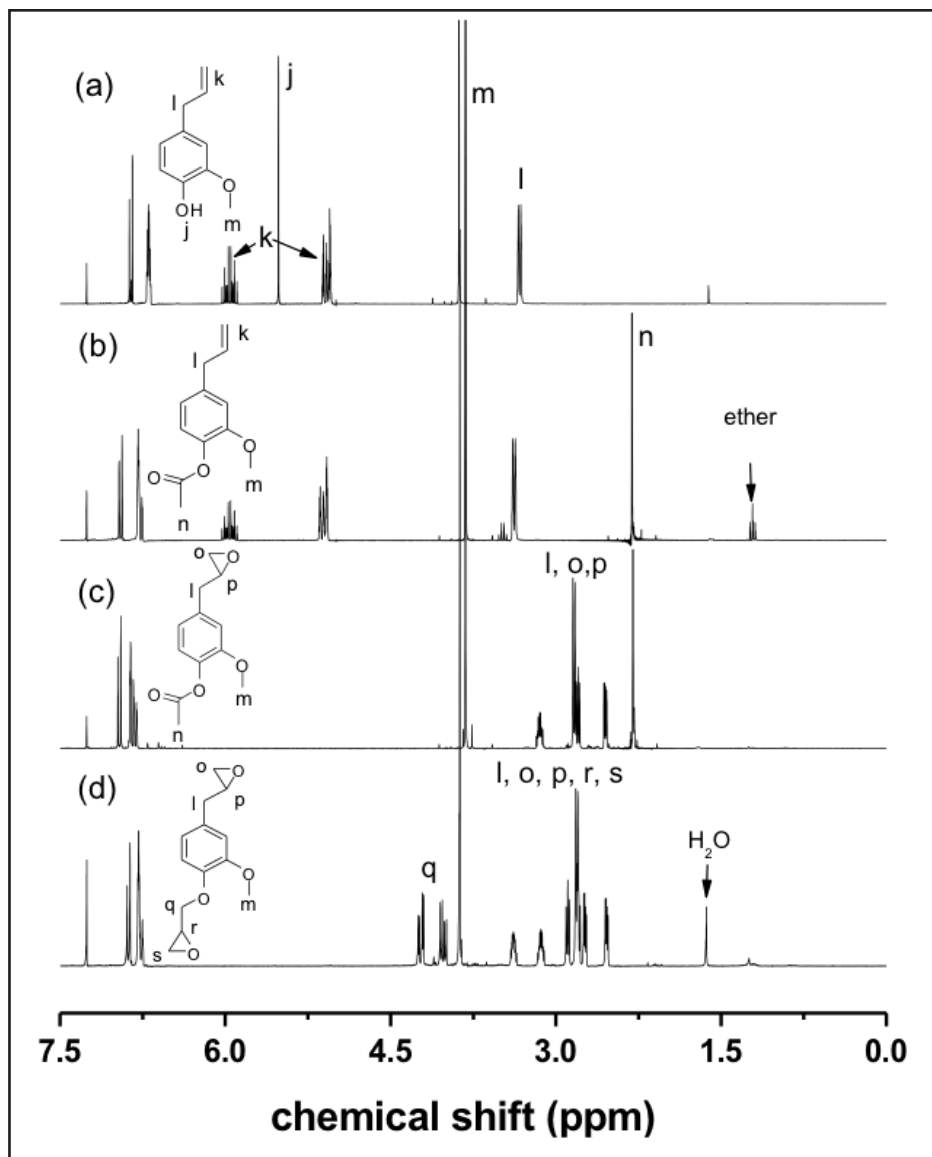


Figure PL-1.1. ^1H NMR spectra of Eu-EP and intermediates at different stages of the synthesis

addition of EMID to Eu-EP/MPA also greatly decreased the curing temperature and resulted in an increase in heat of reaction of almost four times. The multiple peaks are due to different reactions involved in the curing. Based on this result, EMID as catalyst was used in all the rest of the samples for studies of curing kinetics and thermal properties.

Figure PL-1.2 shows the dependence of storage modulus (G') and $\tan \delta$ on temperature for Eu-EP cured with HHPA and MPA. HHPA and MPA cured Eu-EP samples exhibited very similar values of G' in the glassy state, as shown in Fig. LP-1.2; however, the latter demonstrates a significantly higher T_g than the former (155.3 °C versus 114.2 °C). In contrast, DER353 cured only with HHPA exhibited a lower T_g of 106.1 °C. The high T_g of the MPA-cured Eu-EP is likely attributed to the large rigid structure of the rosin moiety. G' of Eu-EP/HHPA at 35 °C (2.8 GPa) is comparable to that of ER353/HHPA (2.9 GPa), and both are slightly higher than that of rosin-derived epoxy (2.5 GPa). Eu-EP/MPA also exhibited a comparable G' of 2.9 GPa at 35 °C but a lower G' in the rubber state than Eu-EP/HHPA. This result is probably due to the high molecular weight of MPA which results in a decrease in crosslink density. Since G' and T_g of Eu-EP/HHPA are comparable with those of DER353/HHPA, Eu-EP may have a great potential as a substitute for some BPA epoxies.

Table PL-1.1. DSC results of non-isothermal curing and thermal stability of the cured eugenol epoxies.

Parameter	Eu-EP/HHPA/EMID		Eu-EP/MPA/EMID		DER353/HHPA/EMID
	1/0.8/0	1/0.8/0.08	1/0.8/0	1/0.8/0.12	1/0.8/0.08
T_g (°C) ^a	214.2	132.7/143.8	230.4	120.0/141.3/152.9	135.7/148.4
ΔH (J g ⁻¹) ^a	237	445	69.9	262	287
E_a (kJ mol ⁻¹)	65.9	65.7/73.4	68.9	63.2/68.1/71.2	60.0/72.5
T_{05} (°C) ^b	-	321.2	-	316.9	341.4
T_g (°C)	-	114.2	-	155.3	106.1
G' (GPa)	-	2.8	-	2.9	2.9

^a measure from curing at a heating rate of 10 °C min⁻¹.

^b Temperature at which 5% weight loss was incurred.

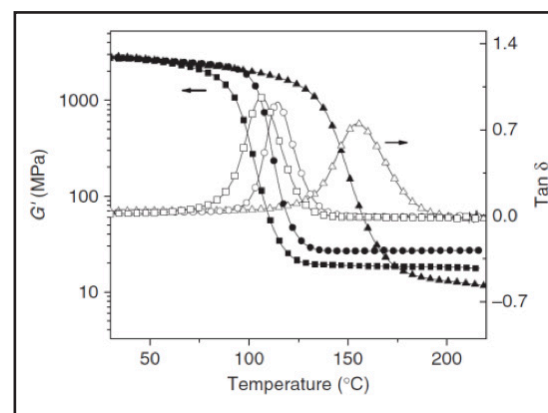


Figure PL-1.2. Dynamic mechanical properties of cured DER353/HHPA (squares), Eu-EP/HHPA (circles) and Eu-EP (triangles)

Conclusions/Discussion

A new epoxy based on the renewable eugenol was successfully prepared by epoxidation of the double bond followed by glycidylation of the phenolic hydroxyl in the eugenol structure. The eugenol epoxy was a solid with a low melting point, and it could be obtained with high purity and an acceptable yield.

When cured with HHPA, the eugenol epoxy and the DER353 BPA-type epoxy exhibited similar curing behavior, dynamic mechanical properties and thermal stability. Furthermore, the eugenol epoxy cured with a rosin-derived anhydride (MPA) exhibited higher T_g than that cured with HHPA. The results from this study indicate that eugenol and rosin are potential feedstocks for epoxy resins, and the cured resins exhibited very comparable performance with respect to that of their petrochemical counterparts.

1.2. Partial depolymerization of lignin via two catalytic methods under mild conditions

Objective

Because a viable lignin-to-chemical technology is still not likely to be realized at time soon, we focus our effort on using lignin itself as feedstock for polymer materials [Wang & Rinaldi, 2012; Zhao et al., 2010]. Specially, biorefinery for the second-generation bioethanol utilizes the easily convertible carbohydrate portions of the lignocellulosics and leaves lignin as a main byproduct. This lignin obtained from the residue of enzymatic hydrolysis of lignocellulosics is assumed close to its original state. Therefore, it will be quite different from KL and organosolv lignin in terms of molecular weight and solubility. This kind of lignin was seldom investigated because it contains lignin fractions of much higher molecular weights compared to Kraft and organosolv lignins. In this task, partial depolymerization of NARA lignin was studied via two depolymerization methods, mild hydrogenolysis under the catalysis of Raney Ni and based-catalytic depolymerization. Since our main objective is to increase the hydroxyl content for functionalization and the miscibility and/or compatibility of the lignin derivatives with other ingredients in thermosets or adhesives, lignin only needs to be partially depolymerized. That means the depolymerization reaction will selectively cleave the less strong aryl-O-aryl and aryl-O-aliphatic linkage and leave benzene ring largely intact. The depolymerized lignins exhibited greatly enhanced hydroxyl values, low molecular weights and narrow distributions.

Methodology

To investigate preparation of partial depolymerization of lignin (PDL) by the BCD approach, we initiated our investigation with KL as a model lignin because of its easy availability, relatively low molecular weight and high hydroxyl content. The conversion of KL to a soluble compound was successful with a yield ~ 70 wt%. In general, BCD was performed with NaOH as catalyst at ~ 250 °C for 90 min in supercritical methanol and the pressure was about 1400 psi. After cooling to room temperature, the reaction solution was adjusted to be neutral and then filtrated. Subsequently, methanol was evaporated and the residue was dissolved in acetone and filtrated again to further remove the salt. The acetone was evaporated, and the product was dried in vacuum oven overnight to obtain PDL. The PDL product was a solid but could be dissolved in some organic solvents like THF, acetone, and methanol. Besides Kraft lignin, NARA lignin was also partially depolymerized by BCD.

Partial hydrogenolysis of four types of lignin samples, NARA DA, CLE (A), CLE (B) and WOx, were investigated. All the hydrogenation reactions were conducted under the catalysis of Raney Ni under mild conditions in a 3% NaOH solution in dioxane/H₂O (1/1, v/v). The reaction was conducted in the pressure reactor with an overhead mechanical stirrer. The reactor was pressurized with H₂ to 2.0 MPa at room temperature and then the reaction was performed at the selected temperatures. The reaction lasted for 3.5 h. After the reactor was cooled to room temperature, Raney Ni was retained at the bottom of the reaction using a magnet while the mixture was decanted and filtered. The residue left at the bottom was washed with a small amount of water and decanted into the funnel. The washing was repeated several times till clean Raney Ni catalyst was recovered. After the filtrate was adjusted to pH = 7.0 with 1N HCl, the product was precipitated, collected by centrifugation and freeze-dried.

Results

As shown in Table PL-1.2, three NARA lignins derived from different pretreatments

Table PL-1.2. Depolymerization of lignins by the BCD method

Samples	Hydrogenolysis Temp.	Yield (%)	OH value (mmol/g)
DA	175 °C	87.8	-
	200 °C	88.8	4.4
	250 °C	75.4	-
CLE (A)	175 °C	66.8	-
	200 °C	80.8	3.8
	250 °C	55.2	-
WO	175 °C	88.0	-
	200 °C	86.0	4.1
	250 °C	61.0	-

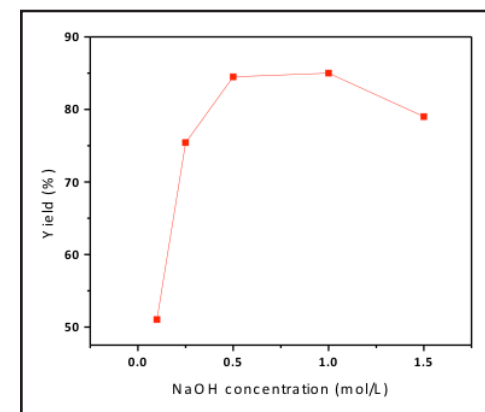


Figure PL-1.3. Effect of NaOH concentration on yield.

were partially depolymerized at different temperatures using BCD method with 1N NaOH solution. The highest yield achieved was ~80% at 200 °C. The hydroxyl value of PDL was greatly improved. Compared to other two lignins, NARA DA lignin showed higher yield and hydroxyl value. The effect of NaOH concentration on yield was also studied (Figure PL-1.3). The yield increased with NaOH concentration. When the concentration was higher than 1.0 mol/L, however, the yield started to decrease because high NaOH concentration probably led to the formation of low molecular weight volatile compounds that were collected. Therefore, the optimum NaOH concentration is around 1.0 mol/L.

Partial hydrogenolysis of DA lignin was also studied. The effects of solvent and various reaction conditions were studied. The yield of the hydrogenolysis conversion was calculated using Equation (1):

$$\text{Yield} = \frac{\text{weight of soluble lignin}}{\text{weight of initial lignin}} \times 100 \quad (1)$$

Table PL-1.3 shows the influences of solvent medium, NaOH and Raney Ni, on hydrogenolysis of NARA DA lignin under mild temperature and pressure. It is known

that solvent plays an important role in hydrocracking of lignin for chemicals. The solvent is to not only dissolve the depolymerized lignin product but also solvate the lignin and facilitate the interactions among catalyst, hydrogen and the substrate during reaction. Depolymerization of lignin was found to be more effective in the presence of alkali (Miller et al., 1999; Shabtai et al., 1999). The mixture of dioxane and H₂O serves as a good solvent for alkali and the depolymerized products. In Table PL-1.3, the catalytic hydrogenolysis in 3% NaOH aqueous solution exhibited a yield of 43.7% (entry 1). Even without use of catalyst, the conversion reached 53.3% when the hydrogenolysis was performed in 3% NaOH solution in the mixed dioxane/H₂O (1/1, v/v) (entry 2). When Raney Ni was added, however, the conversion increased to 70.6% (entry 3). This result clearly suggests the important role of alkali in the reaction. Without NaOH, the reaction in the same mixed solvent only yielded a conversion of 16.7% (entry 4). Hereafter, all the rest hydrogenolysis experiments were performed in the medium of 3% NaOH in dioxane/H₂O (1/1 v/v) and with

Table PL-1.3. Yield obtained from different reaction systems

Entry	Yield/%	Reaction conditions ^a
1	43.7	3% NaOH H ₂ O solution, Raney Ni
2	53.3	3% NaOH in dioxane/H ₂ O (1/1 v/v), (no catalyst)
3	70.6	3% NaOH in dioxane/H ₂ O (1/1 v/v), Raney Ni
4	16.7	No NaOH, in dioxane/H ₂ O (1/1 v/v), Raney Ni

^a lignin/solvent, 15 mg/mL; Raney Ni, 16.7% based on lignin weight; 160 °C; 2.0 MPa and 3.5 h.

Raney Ni catalyst.

In addition to the solvent medium used, effects of other reaction parameters including temperature, catalyst concentration and lignin concentration on hydrogenolysis conversion were also examined. Reaction temperature played an important role in the hydrogenation of lignin. Increasing temperature can usually improve the yield and shorten the reaction time. Figure PL-1.4a shows that the yield increased continuously with temperature increasing from 120 to 180 °C. For the reaction performed at 180 °C, the yield of conversion was ~82%. However, the yield decreased to ~70% when the temperature further increased to 200 °C. Since the solid residue from the same hydrolysis was ~10% on the basis of the starting lignin, the decrease in yield was likely due to the formation of more monomeric chemicals at high temperatures. Most of these monomeric chemicals probably remained soluble in the mixture of dioxane/H₂O after lignin was precipitated. Figure PL-1.4b shows the effect of catalyst content on the yield of conversion of hydrogenolysis at 160 °C, 2.0 MPa and 3.5 h. When the content of Raney Ni increased from 8.3 to 28% (on the basis of lignin weight), the yield continuously increased from 59.1 to 80.0%. At 16.7% Raney Ni, the yield could be as high as 70.6%.

To determine the molecular weight of lignin using GPC, the depolymerized lignin was first acetylated to increase its solubility in THF (Mansouri et al., 2011). Table

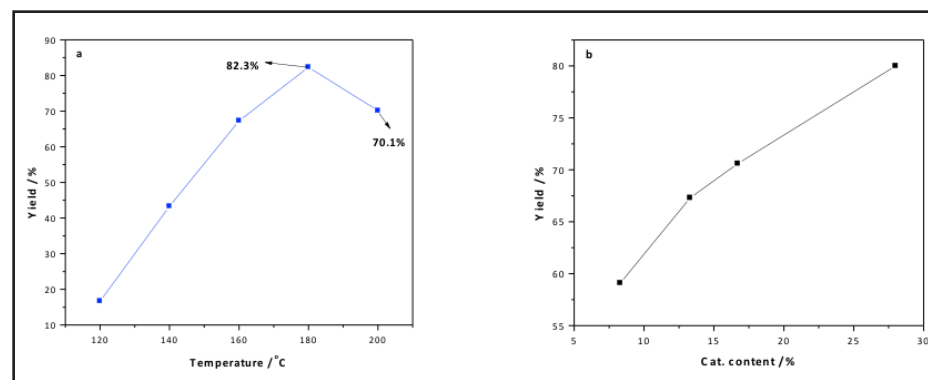


Figure PL-1.4. Effects of temperature (a) and catalyst content (b) on yield of hydrogenation of lignin.

PL-1.4 lists the calculated results of the molecular weight distributions. When the temperature was increased from 140 °C to 160 °C, the depolymerized lignin was given by an average molecular weight (M_w) of ~1522 g/mol and a number average molecular weight (M_n) of ~859 g/mol. As the temperature further increased to 180 and 200 °C, the molecular weight of the resulting product decreased further (Table PL-1.4). It should also be pointed out that all three depolymerized lignin samples hydrogenolyzed respectively at 160, 180 and 200 °C exhibited relatively small

polydispersity (M_w/M_n). This result indicates that hydrogenation under mild reaction conditions can effectively break the bulky structure of lignin into oligomer units.

Hydroxyl value of lignin is a critical factor for its polymer applications. In this study, hydroxyl values of lignin samples were determined using ^{31}P NMR (Figure PL-1.5).

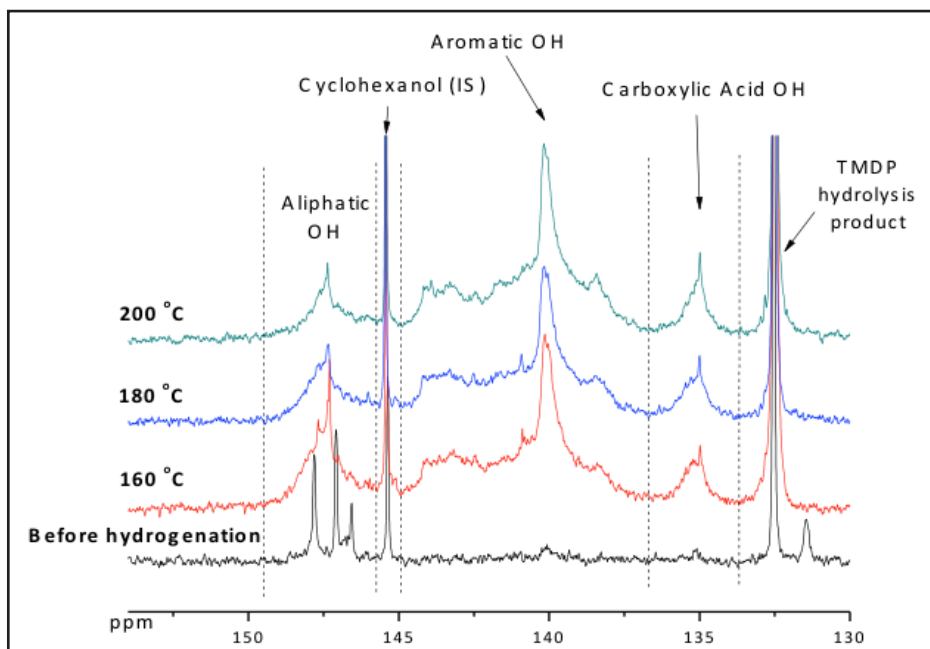


Figure PL-1.5. ^{31}P NMR spectra of before and after hydrogenation of lignin at different temperatures.

Because the original NARA DA lignin was hardly soluble in the mixture solvent ($\text{CDCl}_3/\text{pyridine}$) for ^{31}P NMR analysis, its spectrum shown in Figure PL-1.5 only represented the structure of the soluble portion in the mixture solvent and was not used for quantitative determination of hydroxyl groups. The hydroxyl groups of lignin can be categorized in three groups, aliphatic, aromatic and carboxylic. The calculated hydroxyl values for all three depolymerized lignin samples are

Table PL-1.4. Characterization of the depolymerized lignins by GPC and ^{31}P NMR

Temp. (°C)	Mw (g/mol)	Mn (g/mol)	Mw/Mn	Hydroxyl value (mmol/g)			Total
				Aliphatic ¹	Aromatic ²	Carboxylic ³	
140	1087	99	-	-	-	-	-
160	1522	859	1.77	0.81	2.40	0.37	3.58
180	1368	827	1.65	0.71	2.68	0.44	3.85
200	1100	770	1.43	0.66	3.22	0.50	4.38

^{1, 2, 3} Chemical shift regions: 1. 145.5 - 150.0 ppm; 2. 136.6 - 144.7 ppm; 3. 133.6 - 136.6 ppm

summarized in Table PL-1.4. With hydrogenolysis temperature increasing from 160 to 200 °C, the hydroxyl value of the resulting products increased continuously. The increase was mainly seen in the aromatic hydroxyls, which suggested that the cleavage of ether bonds in lignin occurred effectively. It is believed that the cleavage of α - and β -O-4 bonds which produce the combined *para*-OH- ϕ and guaiacyl (137.5-140.8 ppm) is the predominant process during the hydrogenation in the alkaline medium (Mansouri et al., 2011). The lignin sample hydrogenated at 200 °C exhibited the highest hydroxyl value of 4.38 mmol/g, which could be a good raw material for lignin-based epoxy resins.

The solubility of PDL in organic solvent is very important for its modification reaction, like acetylation, methylation, glyoxalation, epoxidization, etc. The dissolutions of NARA DA lignin before and after hydrogenolysis at 180 °C in THF, DMSO, pyridine and 3% NaOH dioxane/ H_2O were compared by diffusion test on filter paper. In Figure PL-1.6a, the original lignins suspended in all the selected solvents apparently accumulated in the center of the halomarks (upper row), suggesting the insolubility. On the contrary, the hydrogenolyzed lignins in all four solvents left well-diffused halomarks, indicating the lignin was soluble or at least was finely dispersed in the solvents. After being kept overnight, the mixtures of the original lignins in all four solvents stratified apparently (Figure PL-1.6b). In contrast, the hydrogenolyzed lignins still appeared as stable solutions.

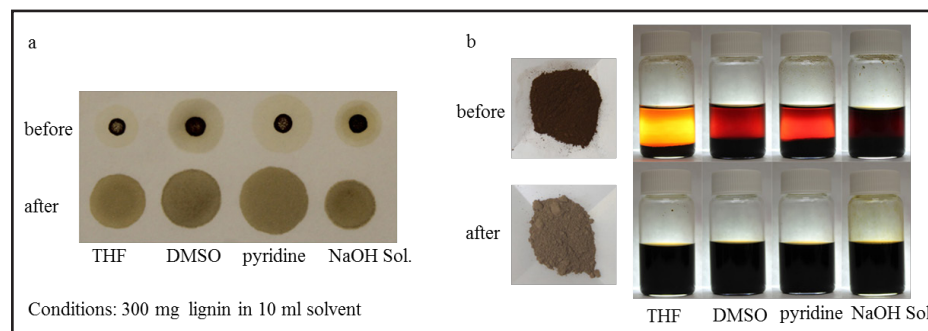


Figure PL-1.6. Comparisons of solubility of lignins between before (a) and after hydrogenolysis (b).

Conclusions/Discussion

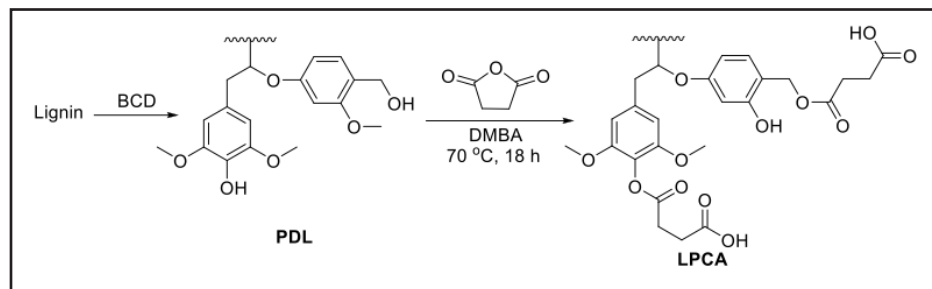
In summary, two depolymerization methods, BCD and hydrogenolysis, both partially depolymerize NARA lignin effectively. The BCD method produced the PDL with more hydroxyl value and gave high yield especially for NARA lignin, but this method used higher NaOH concentration and higher reaction temperature than the hydrogenolysis method. Partial hydrogenolysis of NARA lignin was successfully performed under the catalysis of Raney Ni and mild conditions. The hydrogenolysis

of NARA DA gave PDL of higher yield but lower hydroxyl value. The PDL prepared by hydrogenolysis exhibited good solubility/dispersability in THF, dioxane, pyridine and 3% NaOH solution. Having good solubility/dispersability in organic solvent is very helpful for further modification of NARA lignin like epoxidation, ammoxidation or oxidation through which lignin is converted into effective building blocks for engineering polymers.

1.3. Synthesis of curing agents using PDL from BCD method

Objective

Direct use of the polymeric lignin rather than lignin-derived monomeric chemicals as a building block in new polymer synthesis, either in the form unmodified or partially depolymerized lignin, is worth more attention and likely results in viable applications. We have made a great effort in the past years to explore the BCD liquefaction process of lignin in supercritical organic solvents [Qin et al. 2014]. This process is also called high-pressure direct liquefaction, which is in fact a cracking treatment. Unlike fast pyrolysis, liquefaction in supercritical solvent requires much milder reaction conditions, and lignin is largely depolymerized but is not degraded to the level of monomeric chemicals. As a result, gasification and charring do not occur and most lignin is converted to solvent soluble products. In this subtask, the cracked lignin by the above BCD method was used for preparation of lignin derived carboxylic polyacid (LPCA) and its application as curing or co-curing agent for epoxy resin was studied. As shown in Scheme PL-1.2, lignin was first cracked through base catalyzed depolymerization to increase its solubility, and then the carboxylic acid groups were attached to cracked lignin by reacting PDL with succinic anhydride to obtain LPCA. Subsequently, LPCA was used as curing agent to cure commercial epoxy of DER 353. The aim of this task was to explore the application of lignin as more effective and reactive component in epoxy.



Scheme PL-1.2. Preparations of lignin derived carboxylic polyacid (LPCA).

Methodology

The PDL was prepared using the method described in section 2.1 of this report. The resulting PDL remains solid but is readily soluble or dispersible in organic solvents. PDL also has an increase in hydroxyl groups available for reactions. The approach to introduce carboxylic acid groups to the structure of lignin is to react PDL with succinic anhydride as shown in Scheme PL-1.2. PDL and succinic anhydride in a weight ratio of 1:0.7 with N, N-dimethylbenzylamine (DMBA) as catalyst were reacted in acetone at 70 °C for 6 h. The product was collected after evaporating acetone under vacuum. The LPCA obtained was a black solid at room temperature and became liquid at temperatures above 70 °C. Glycerol was also reacted with succinic anhydride similarly to prepare glycerol-derived triacid (called as GTA). Curing of DER 353 using the LPCA as a curing or co-curing agent was studied. In addition, 2-ethyl-4-methylimidazole was used as a catalyst and added at 1% on the total weight of epoxy and curing agent.

Results

After partial depolymerization in supercritical methanol, the resulting PDL had a hydroxyl value of 7.15 mmol/g. Moreover, the PDL was soluble in a variety of solvents, which would make functionalization reactions more effectively in solution reactions. Figure PL-1.7 (a) shows the ^{31}P NMR of PDL. It was noted that most of the hydroxyl groups of PDL had reacted with succinic anhydride to form succinate monoesters, meaning that free carboxylic acid groups were introduced to PDL. The acid value of LPCA was found to be 229 g/mol by comparing the peak areas of the acid and internal standard. There was a small amount of unreacted hydroxyl groups in the product because the hydroxyl groups were in slight excess during the reaction. Figure PL-1.7 (b) shows the FT-IR spectra of lignin, PDL, LPCA, and the LPCA cured DER353. Compared to the spectrum of lignin, the absorption of the carbonyl groups in PDL at 1700 cm^{-1} increased, indicating some carbonyl groups were formed during the BCD process. After PDL was reacted with succinic anhydride, the resulting LPCA

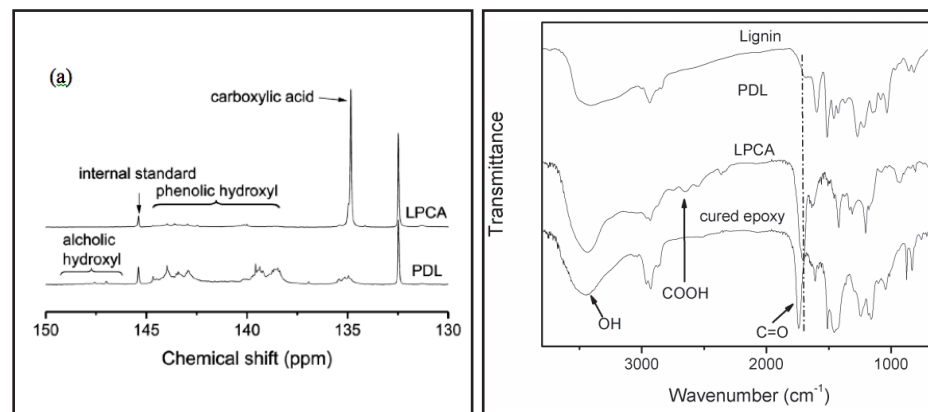


Figure PL-1.7. ^{31}P NMR of PDL and LPCA (a) and FTIR spectra of lignin and derivatives (b)

exhibited another great increase in the absorbance at 1700 cm^{-1} . At the same time, a new peak appeared at 2700 cm^{-1} , suggesting that the product contained a lot of carboxylic acid groups.

Curing of DER 353 and LPCA in different equivalent ratios with 1 wt % EMID on the basis of total weight of resin was studied using DSC. Figure PL-1.8 shows that the curing for all formulations started and peaked at similar temperatures ($\sim 145\text{ }^\circ\text{C}$). However, when the ER353/LPCA ratio was 1/0.6, another peak appeared at a higher temperature ($\sim 165\text{ }^\circ\text{C}$). This result indicated there were probably two types of reactions involved because of the shortage of carboxylic acid groups. When the DER353/LPCA ratio was 1/0.8, a broad exothermic peak was noted in the DSC thermogram. As the equivalent of LPCA increased further in the formulation, i.e., at the DER353/LPCA ratio of 1/1, the exothermic peak of curing narrowed slightly. This

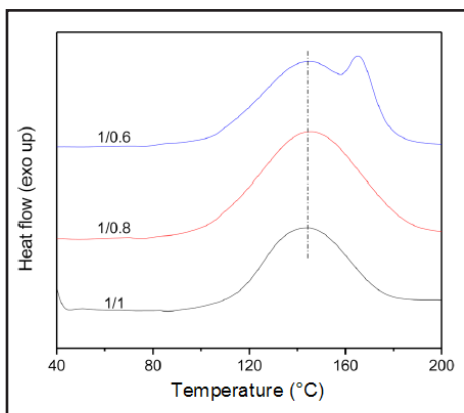


Figure PL-1.8. DSC curves of DER 353/LPCA with different ratios

result might suggest that in the latter two cases the curing involved only one major reaction, i.e., the reaction of the carboxylic acid group and epoxide. In Figure PL-1.7 (b), the absorption of carbonyl groups of the unreacted LPCA at 1700 cm^{-1} shifted to 1740 cm^{-1} in the cured DER353/LPCA (1/1) and the peak of carboxylic acid groups at $\sim 2700\text{ cm}^{-1}$ disappeared. This FTIR result indicates that the carboxylic acid group reacted with the epoxy groups to form ester bonds.

Figure PL-1.9 shows the dynamic mechanical properties of the LPCA cured DER353. As the DER353/LPCA equivalent ratio varied from 1/0.6,

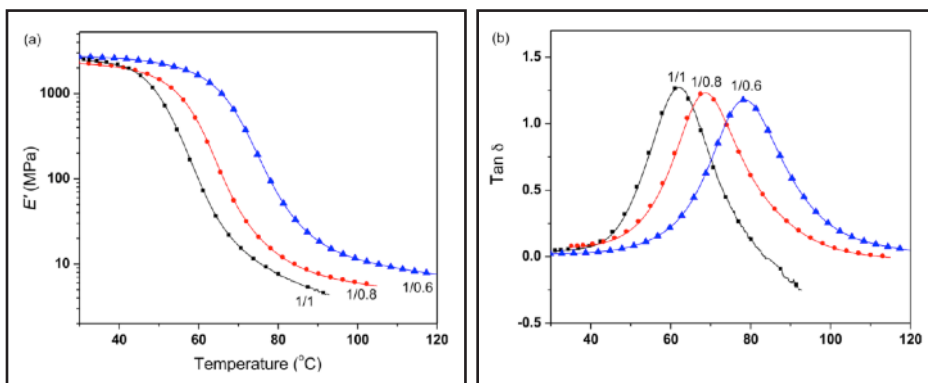


Figure PL-1.9. Storage modulus (a) and $\tan \delta$ versus temperature for DER353/LPCA with different ratio

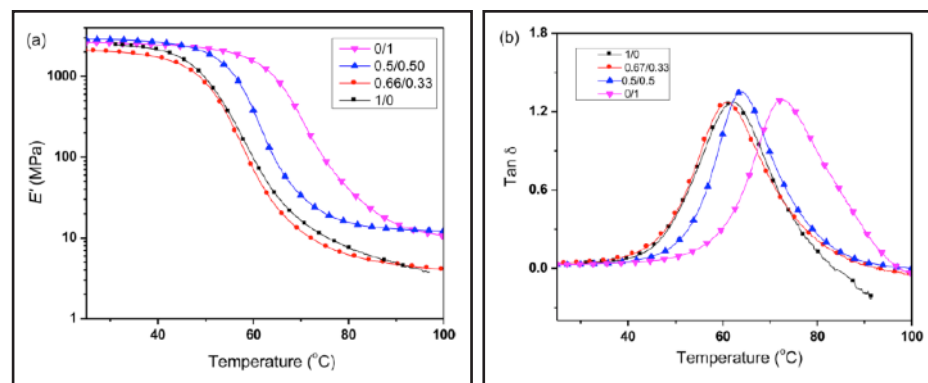


Figure PL-1.10. Storage modulus (a) and $\tan \delta$ versus temperature for DER353 resin cured with LPCA/GTA

1/0.8, to 1/1, the T_g of the cured resins decreased from 78.5 , 69.4 , to $62.3\text{ }^\circ\text{C}$, while the storage moduli (E 's) at room temperature were comparable (2.4 - 2.7 GPa). The introduction of the linear succinate monoester enhanced the flexibility of the lignin molecules. Therefore, increasing the content of curing agent (LPCA) in the formulation tended to reduce the T_g of cured resins. On the other hand, lignin contents in these three samples were 24.8 , 29 , and 32.3% , respectively.

Because LPCA was solid, liquid co-curing agents were selected to reduce the viscosity of the resin system. Because LPCA cured epoxies only exhibited some moderate T_g s, the selected co-curing agent was also intended to increase the T_g and stiffen the cured resins. In this task, GTA or HHPA was used as co-curing agent with LPCA to cure DER353. In all formulations, the epoxy and the total curing agent were in equal equivalents. Figure PL-1.10 shows the dynamic mechanical properties of the DER 353 cured with LPCA/GTA. It was noted that at different LPCA/GTA ratios the storage moduli (E 's) of cured epoxy resins were comparable.

Meanwhile, the T_g s of the epoxies cured by LPCA/GTA also showed little difference since the DER 353 cured by 1 equiv GTA was just $10\text{ }^\circ\text{C}$ higher than that cured by 1 equiv LPCA. The T_g s of the cured epoxies at different curing agent ratios, are listed in Table PL-1.5. GTA seemed to render the cured epoxy a higher cross-link density than LPCA, as evidenced by the higher E' in the rubbery state. In contrast, use of HHPA as a co-curing agent increased the T_g of the cured resins gradually (Figure PL-1.11) because of the rigid molecular structure and low molecular weight of HHPA. The HHPA cured epoxy exhibited a T_g of $\sim 110\text{ }^\circ\text{C}$, being the highest among all cured epoxies. Figure PL-1.11 also shows that the E' of LPCA cured DER 353 was very similar to that of the pure HHPA cured one. The E' for the epoxy cured with 1 equiv LPCA was 2.44 GPa at $30\text{ }^\circ\text{C}$ and was comparable to that of the HHPA cured DER 332 and some other biobased epoxies reported in our previous study [Liu et al. 2009; Qin et al. 2014b].

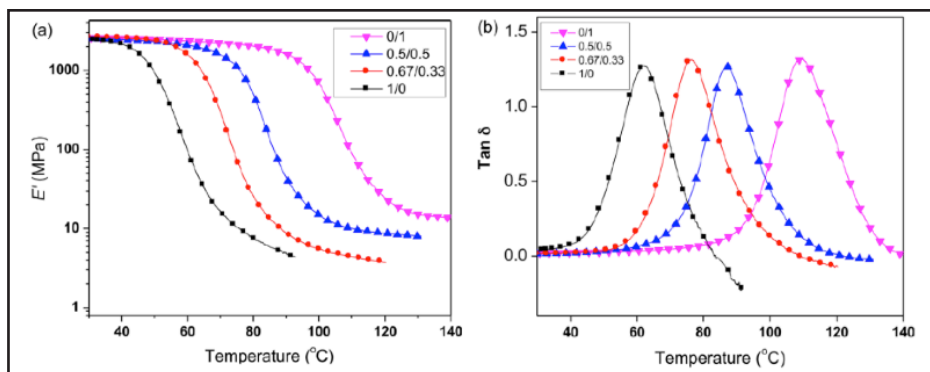


Figure PL-1.11. Storage modulus (a) and $\tan \delta$ versus temperature for DER353 resin cured with LPCA/HHPA

Table PL-1.5. Effect of co-curing agents on T_g and thermal stability of the cured epoxy resins

Co-curing agent and equivalent	LPCA	LPCAs/GTA			LPCAs/HHPA		
	1	0.67/0.3	0.5/0.5	0/1.0	0.67/0.33	0.5/0.	0/1
T_g (°C)	62.3	60.5	63.8	72.3	76.4	85.3	109.9
T_{d5} (°C)	269.3	302.8	302.3	301.4	282.0	297.2	339.0

Thermal stability of the cured samples was also measure by TGA. The temperatures at which 5% weight loss was incurred, T_{d5} are also listed in Table PL-1.5. It is noted that T_{d5} of the LPCA cured epoxy was 269.3 °C. With GTA as a co-curing agent, the T_{d5} increased to ~300 °C. This increase in thermal stability was possibly due to the increased cross-linking density caused by the higher functionality of GTA. When HHPA was used as a co-curing agent, the thermal stability increased gradually with HHPA content.

Conclusions/Discussion

Base-catalyzed depolymerization at mild conditions could partially depolymerize lignin, resulting in improved solubility in organic solvent. The resulting PDL was successfully converted to lignin-based polycarboxylic acid (LPCA) by reacting with succinic anhydride. LPCA could act as a curing or co-curing agent in the preparation of epoxy resins. It was noted that LPCA could act as a curing agent to cure a commercial epoxy (DER 353) in a similar temperature range as the commercial anhydride type curing agents. The LPCA cured DER 353 resin exhibited a moderate T_g and comparable storage modulus to that cured with a commercial anhydride curing agent. The solid LPCA could be used together with other liquid curing agents such as glycerol tris(succinate monoester) (GTA) and commercial hexahydrophthalic anhydride (HHPA) to cure epoxies. The result indicated that use of mixture of LPCA

and a liquid curing agent not only adjusted the viscosity of the resin system but also greatly regulated the dynamic mechanical properties and thermal stability of the cured resins. This work demonstrates that partially depolymerized lignin can serve as a feedstock in the preparation of curing agent and be used for epoxy applications.

1.4. Preparation of PDL based epoxies/curing agents and application development for PDL-based epoxy asphalt

Objective

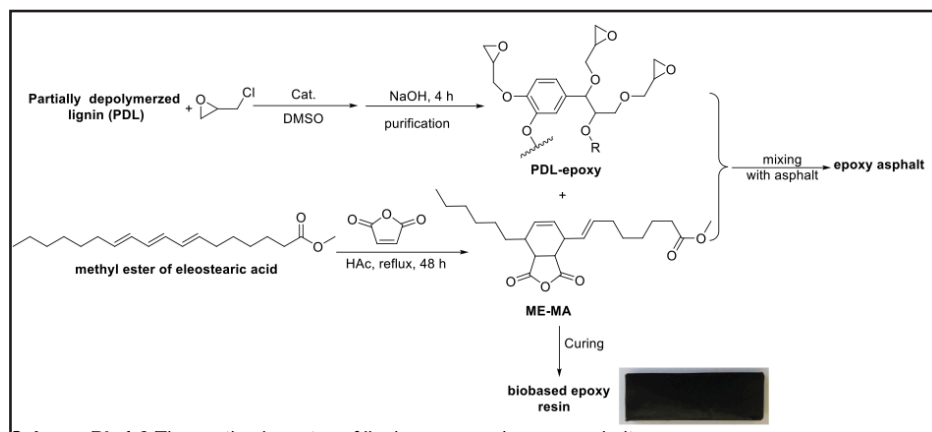
The phenolic and alcohol hydroxyls present in lignin make it an attractive reactive ingredient to be incorporated into thermosetting resins [Yin & Di, 2012; Li & Ragauskas, 2012a; Li & Ragauskas, 2012b]. However, the highly branched molecular structure makes these hydroxyls less accessible for derivatization and the resulting lignin derivatives immiscible in the resin system, giving poor end-use performance. In section 2.1, we demonstrate that lignin can be partially depolymerized over Raney Ni under mild conditions [Xin et al., 2014]. The partial depolymerized lignin (PDL) has increased solubility in organic solvent and increased hydroxyl content from both phenolic and aliphatic hydroxyl groups. This partial destruction of lignin bulky structure releases more hydroxyl groups for reactions and is miscible or compatible with other ingredients in the thermoset system. Lignin and lignin derivatives have found some applications in asphalt products. For example, cationic surfactants derived from lignin were used to prepare asphalt emulsion [Liu et al. 2013]. The asphalt binder is always subjected to a wide temperature variation from season to season and great stress from heavy truck traffic, and it is likely to crack in the cold winter and lose its cohesive strength in the hot summer months. In order to improve the temperature-resistance properties of asphalt, one approach is to modify the asphalt binder with the incorporation of epoxy resin, which can greatly improve performance of the asphalt binder especially at higher temperatures. Current epoxies used for asphalt modification are all petroleum based and mostly bisphenol A (BPA) type epoxy resins [Yu et al., 2009; Cong et al., 2010; Xie et al., 2011]. PBA type epoxies are generally expensive and are also suspicious chemical estrogen. Therefore, there is a great interest in developing alternative epoxies.

In this task, we studied the modification of asphalt binder using lignin-derived epoxy. NARA lignin used for this task was partially depolymerized, and then the resulting PDL was converted to a lignin-based epoxy monomer or curing agent. Asphalt was formulated with PDL-epoxy resin in different proportions. The effects of epoxy resin content on the performance of epoxy asphalt mixture were evaluated.

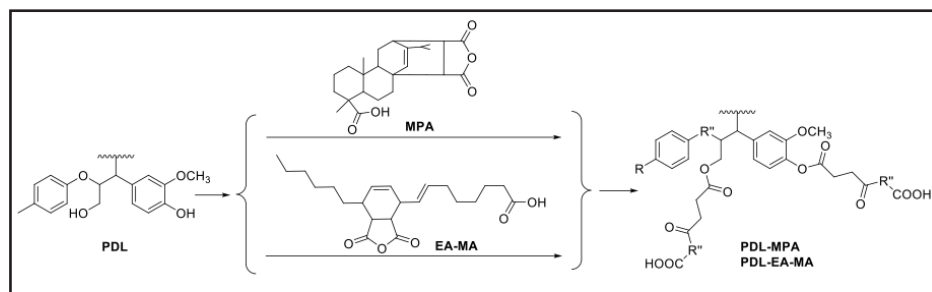
Methodology

The PDL based-epoxy monomer was prepared by reacting epichlorohydrin (ECH) and PDL. Scheme PL-1.3 shows the synthesis route of PDL-epoxy. In brief, after PDL, epichlorohydrin, benzyltriethylammonium chloride and dimethylsulfoxide were charged to a flask, the temperature was raised to 70 °C (or 117 °C) and then the reaction was continued for 3 h. After the reaction mixture was cooled to 60 °C, 1.23 g sodium hydroxide was charged. The mixture was stirred at 60 °C for 4 h. The crude product was washed with ethyl ether twice and then washed by deionized water twice. The product was dried by freeze-drying. Thereafter, these two PDL-epoxies prepared at different reaction temperatures are referred as PDL-epoxy-70 °C PDL-epoxy-117 °C.

Two biobased anhydrides, maleopimaric acid (MPA) and maleated tung acid (EA-MA), were chosen to modify PDL for the preparation of PDL-based curing agents. As shown in Scheme PL-1.4, the resulting PDL curing agent contained multiple carboxylic groups. The preparation procedure is as follows. PDL, maleated rosin or maleated tung acid, dimethyl benzylamine (catalyst) and acetone were added into the flask, and then the temperature was raised to 70 °C. The reaction was continued for 18 h under stirring. After reaction, acetone was removed by



Scheme PL-1.3. The synthesis routes of lignin-epoxy and epoxy asphalt.



Scheme PL-1.4. Preparation of PDL based curing agents.

rotatory evaporation. The residue was washed by ethyl ether, acetone and water successively, and then freeze dried. Yields were 87.5% (PDL-MPA) and 81.7% (PDL-EA-MA) based on PDL, respectively.

In all formulations of the epoxy samples, epoxy and curing agent were maintained in a weight ratio of 1:0.88 for PDL-epoxy/EA-MA and 2:1 for DER332/PDL-MPA or PDL-EA-MA. 2-ethyl-1-4-methylimidazole (EMID) was used as a catalyst and added at 1.0 wt% on the basis of the total weight of curing agent and epoxy. The ingredients were mixed at 70 °C to form a homogeneous mixture, and then the mixture was transferred into an aluminum mold with the dimensions of the cavities being 30 mm × 18 mm × 5 mm. Curing was performed at 150 °C for 2 h and then at 200 °C for 1 h. The cured samples were carefully removed from the mold and used for study of thermal properties.

For the preparation of epoxy modified asphalt, neat asphalt was first heated at 90 ± 5 °C in an oven for 30 min. The premixed epoxy and 1 wt% catalyst EMID was combined with the neat asphalt at different concentrations, i.e., 7.5 wt%, 15 wt% and 22.5 wt% respectively. The samples were cured at 150 °C for 2 h and then 200 °C for 1 h. The resulting epoxy asphalt samples were used for the rheological test.

Results

Epoxy resin prepared from PDL-epoxy monomer and EA-MA

PDL-epoxy was synthesized by the traditional glycidylation method through the reaction of PDL and epichlorohydrin (ECH) (Scheme PL-1.3), and the reaction was conducted at 70 or 117 °C. Initially, like in the usual glycidylation reaction, the reaction was conducted in the presence of ECH, which acted as both reactant and solvent in the first step of the reaction. However, PDL exhibited a poor solubility in ECH and the resulting products were hardly soluble in any solvents. Since the product obtained this way was not soluble in the mixture solvent (CDCl_3 /pyridine), ^{31}P NMR analysis could not be performed to determine the functionality. Because of poor solubility, it was also difficult to determine the epoxy value of these products utilizing the titration method in solutions. This result suggests that glycidylation of PDL without a suitable solvent is of low reaction efficiency. As described in the previous segment, “Partial depolymerization of lignin via two catalytic methods under mild conditions”, DMSO is a good solvent for PDL. When DMSO was used as a co-solvent in the glycidylation, the yields of PDL-epoxy were 86.6% at 70 °C and 100% at 117 °C, respectively. This result suggests that high temperature is beneficial to complete the glycidylation reaction. The obtained PDL-epoxies exhibited good solubility in the mixture solvent (CDCl_3 /pyridine). For the remaining experiments, the PDL-epoxy samples were all prepared by this method with DMSO as a co-solvent.

Figure PL-1.12 shows the FTIR spectra of PDL, PDL-epoxy-70 °C and PDL-epoxy-117 °C. All samples exhibited a broad -OH band at 3470 cm⁻¹, an intense C-H band at 2930 cm⁻¹, a carbonyl peak at 1700 cm⁻¹, the aromatic skeletal vibration at 1600 cm⁻¹ and 1506 cm⁻¹, and the C-H deformations band of asymmetric methyl and methylene appeared at 1460~1470 cm⁻¹. Specifically, a new peak at 908 cm⁻¹ attributed to the oxirane ring was noted in the spectra of PDL-epoxy-70 °C and PDL-epoxy-117 °C. The FTIR results suggest that PDL could be successfully converted to PDL-epoxy.

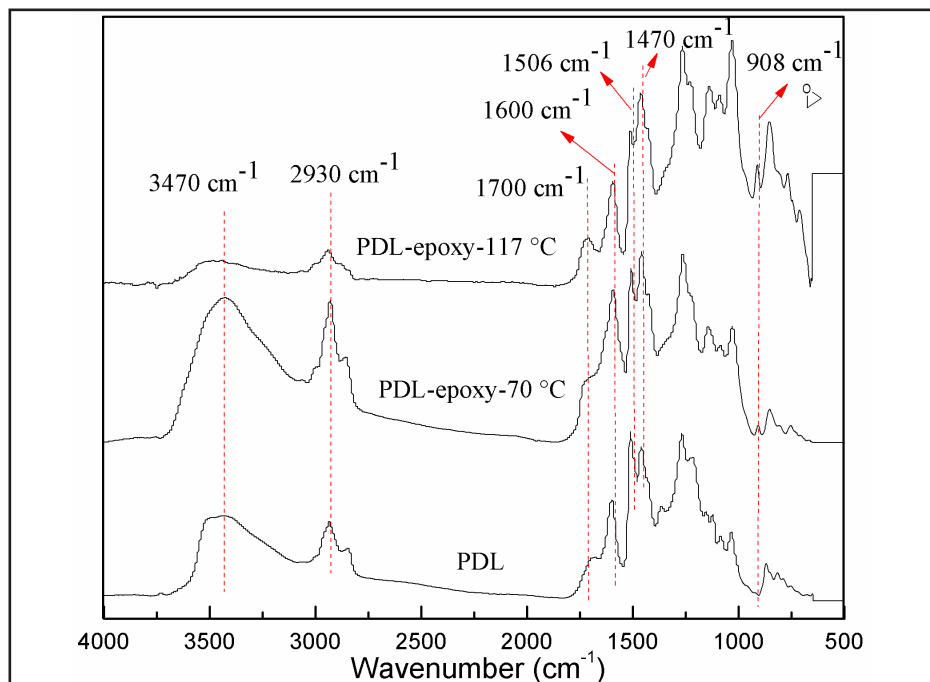


Figure PL-1.12. The FTIR spectra of PDL, PDL-epoxy-70 °C and PDL-epoxy-117 °C.

Figure PL-1.13 shows the ³¹P NMR spectra of the PDL and the two PDL-epoxies. There are three types of hydroxyl groups in these samples, aliphatic, aromatic and carboxylic. The hydroxyl value for each type of hydroxyl was determined by comparing the respective peak area to that of the internal standard. The results of different hydroxyl values for these samples are summarized in Table PL-1.6. By comparing the spectra of the original PDL and PDL-epoxies (Figure PL-1.13), it is noted that the signal of the aromatic hydroxyls of PDL-epoxies in the region of 136.6-144.7 ppm became very weak in PDL-epoxy-70 °C and almost disappeared in PDL-epoxy-117 °C. The signal of the carboxylic acid hydroxyls in the range of 133.6-136.6 ppm disappeared in the spectra of both PDL-epoxy-70 °C and

PDL-epoxy-117 °C. On the contrary, the intensity of the aliphatic hydroxyls with chemical shifts of 145.5-150.0 ppm became strong in PDL-epoxies. As shown in Table PL-1.6, the hydroxyl value of aromatic OH decreased from 3.7 mmol/g in PDL to 1.7 mmol/g for PDL-epoxy-70 °C and to ~0 mmol/g for PDL-epoxy-117 °C. This result suggests that the phenolic hydroxyl groups were fully reacted with ECH when reaction temperature was increased from 70 °C to 117 °C. The signal for carboxylic acid hydroxyls disappeared in the spectra of both PDL-epoxies (hydroxyl value ~0 mmol/g), indicating that the carboxylic acid group has high reactivity in reacting with ECH even at a temperature of 70 °C. However, the aliphatic OH value increased greatly from 0.7 mmol/g in original PDL to 2.4 mmol/g in PDL-epoxy-70

Table PL-1.6. Hydroxyl values of PDL and PDL-epoxies determined by ³¹P NMR

	Hydroxyl value (mmol/g)			Total
	Aliphatic	Aromatic	Carboxylic	
PDL-epoxy-117 °C	2.7	0	0	2.7
PDL-epoxy-70 °C	2.4	1.7	0	4.1
PDL	0.7	3.7	0.3	4.7

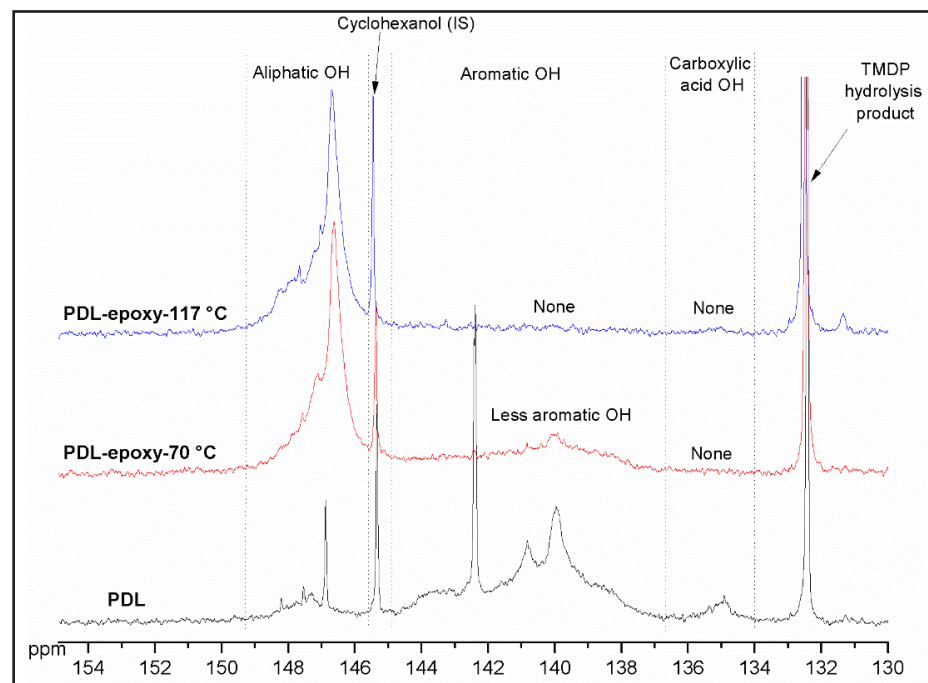


Figure PL-1.13. ³¹P NMR spectra of PDL and PDL epoxies.

°C and 2.7 mmol/g in PDL-117 °C. There are a few possible reasons accountable for this increase. During the glycidylation of lignin the unreacted OH group may react with the previously introduced epoxy ring, resulting in free formations of an ether linkage and an aliphatic OH group. Glycidylation is a two-step process, the ring opening of the epoxide of ECH and with dehydrochlorination that follows. If somehow the second step is not completed, an aliphatic hydroxyl group is also left in the product. After all, the ^{31}P NMR result proves that PDL-based epoxies were successfully synthesized by the conventional method using ECH and a higher reaction temperature promoted the conversion of more hydroxyl groups to epoxy monomers. In the following preparation of epoxy resin, PDL-epoxy-117 °C was used for the study of curing behavior and its thermal properties.

Figure PL-1.14 (a-d) shows the DSC thermograms of the curing of PDL-epoxy and commercial DER332 at different heating rates with the plots of $1/(T_p)$ versus $\ln(\phi)$. The curing of PDL-epoxy exhibited a much broader exothermic peak than the curing of DER 332. This result was because PDL-epoxy has a much more complicated chemical structure in which the epoxies groups likely differ in reactivity. In contrast, the two epoxy groups in DER 332 have the same reactivity toward reacting with

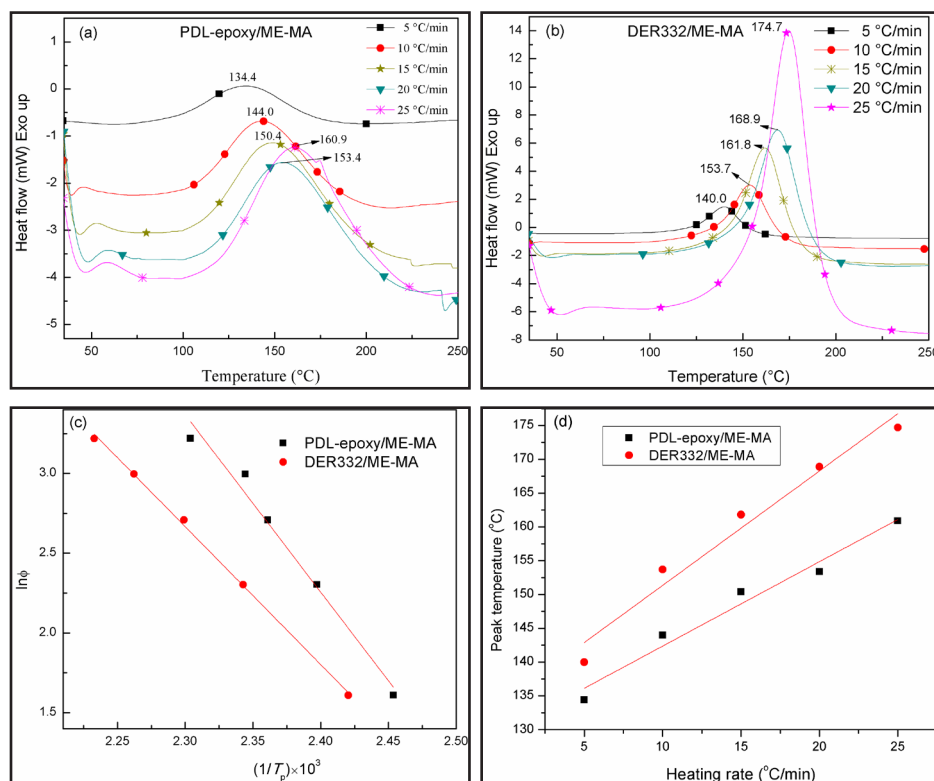


Figure PL-1.14. Comparisons of the non-isothermal curing of the PDL-epoxy and DER 332 at different heating rates (a, b) and the plots of $1/(T_p)$ versus (c, d).

the curing agent. The peak exothermic temperature (T_p) typically shifted to higher temperature with heating rate (ϕ). The calculated curing temperature at zero heating rate was obtained by extrapolating the results to the point of an infinitely slow heating rate and could be used as a reference in the selection of an isothermal curing temperature. The calculated T_p at the zero heating rate for PDL-epoxy/ME-MA was 129.9 °C, which was slightly lower than that (134.4 °C) for DER332/ME-MA (Table PL-1.7). On the other hand, the calculated E_a from Ozawa method for the curing of PDL-epoxy/ME-MA was 87.7 KJ/mol, which was notably higher than that for the curing of DER332/ME-MA (68.3 KJ/mol). Therefore, PDL-epoxy displayed lower reactivity in curing with ME-MA than DER332. This was probably because PDL-epoxy is a solid powder, which would require more energy to enable the curing process.

Table PL-1.7. DSC results of non-isothermal curing and thermal properties of cured epoxies

Epoxy	T_p (°C) ^a	E_a (KJ/mol)	T_g (°C) ^a	V_e ($\times 10^3$ mol/mm ³)	$T_{5\%}$ (°C) ^b	$T_{10\%}$ (°C) ^b	Char yield at 585 °C
PDL-epoxy/ ME-MA	129.9	87.7	94.3	3.02	272.3	311.1	34.7 %
DER332/ME-MA	134.4	68.3	36.1	0.46	219.8	289.9	6.43 %

^a Linear extrapolation at $\phi = 0$
^b $T_{5\%}$ and $T_{10\%}$: temperature of 5% degradation and 10% degradation.

Figure PL-1.15 shows storage modulus (E') and damping ($\tan \delta$) as functions of temperature for PDL-epoxy and DER332 epoxy resins cured with ME-MA. The glass transition temperatures (T_g s) of the cured samples were determined from the peak temperatures of the $\tan \delta$. The V_e of the cured epoxy resin is estimated using the following equation based the theory of rubber elasticity: where E is the elastic modulus of the thermoset in the rubbery state, R is the gas constant and T is the absolute temperature.

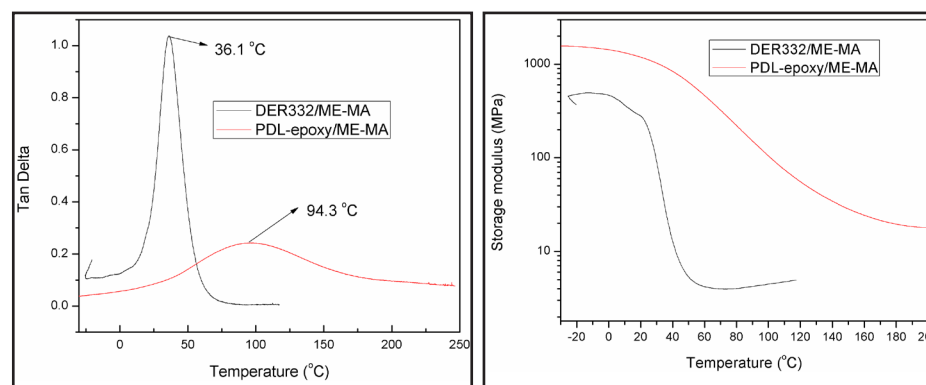


Figure PL-1.15. Storage modulus and $\tan \delta$ versus temperature for DER332 and PDL-epoxy cured with ME-MA.

Since measuring the elastic modulus of thermoset in rubbery state is a very tedious experiment, it is a convenient mechanism to use E' in the rubbery state, e.g., at $T_g + 50^\circ\text{C}$, to substitute E in the calculation. The cured PDL-epoxy resins had higher E' at room temperature than that of the cured DER332 resin. This was probably because the PDL-epoxy had a more bulky structure than DER332, therefore resulting in resins with greater rigidity at room temperature. In Table PL-1.7, it is noted that the T_g and the crosslinking density of the PDL-epoxy resin were higher than that of the DER332 resin. It is understood that more rigid chain segments lead to a higher T_g .

Figure PL-1.16 illustrates the comparison of weight loss as a function of temperature during the TGA experiment for the cured resins. The char yield at 585°C and the temperatures at which 5% weight loss ($T_{5\%}$) and 10% weight loss ($T_{10\%}$) were incurred are summarized Table PL-1.7. These two cured resins showed very similar weight loss behaviors in the initial stage. PDL-epoxy/ME-MA had higher $T_{5\%}$ and $T_{10\%}$ values than DER332/ME-MA. On the other hand, the char yield of PDL-epoxy/ME-MA at 585°C was also obviously higher than that of DER332/ME-MA. These results indicate that the thermal stability of PDL-epoxy was almost as good as that of epoxy resins based on bisphenol A.

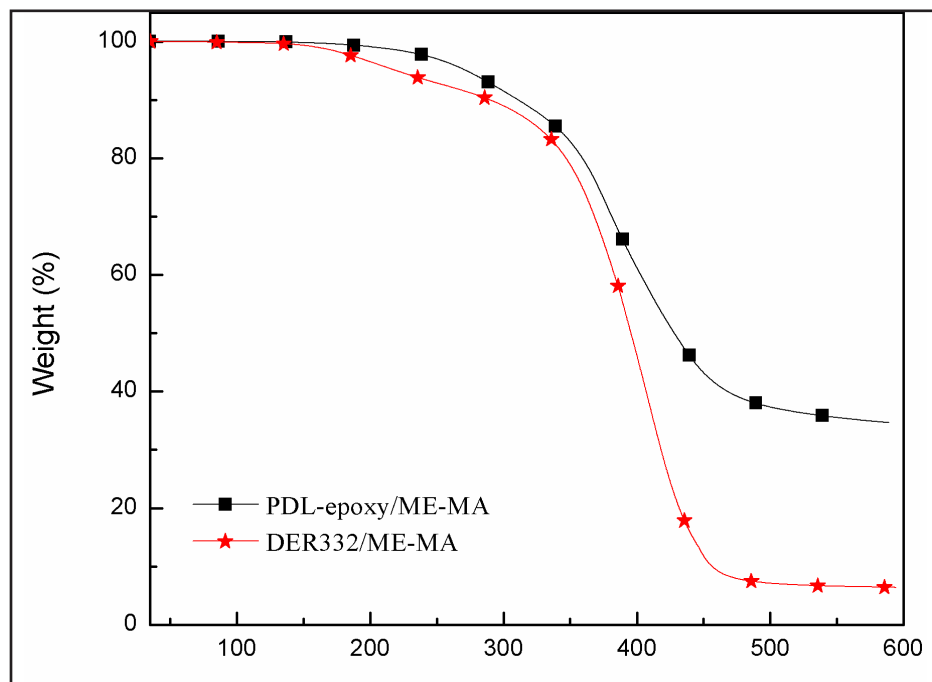


Figure PL-1.16. Comparison of thermal stability of cured PDL-epoxy and DER 332 resins.

1.5. PDL-curing agent

The two synthetic curing agents were characterized by FTIR (Figure PL-1.17). All samples exhibited the typical FTIR absorption peaks of lignin structure. Compared with the spectrum of original PDL, the spectra of PDL-EA-MA and PDL-MPA showed three big differences. First, the broad band around $3460\text{--}3480\text{ cm}^{-1}$ attributed to the stretching of the phenolic and aliphatic hydroxyl groups decreased greatly. This result indicates that most of hydroxyl groups were reacted with the anhydrides groups from EA-MA and MPA. Second, the absorption intensity of carbonyl groups at 1695 cm^{-1} also increased in the spectra of PDL-EA-MA and PDL-MPA. Especially, there was an apparent absorption peak at 1776 cm^{-1} in the spectrum of PDL-MPA that was attributed to the carbonyl group from esters which was newly formed from the reaction between hydroxyl and anhydride groups. Third, a new peak at 921 cm^{-1} in the spectra of PDL-curing agents appeared, which was attributed to C-O-H deformation vibration from carboxylic acid. The FTIR results suggest that PDL was successfully reacted with two anhydride agents through the proposed method and converted to PDL-based curing agents with multi carboxylic acid groups.

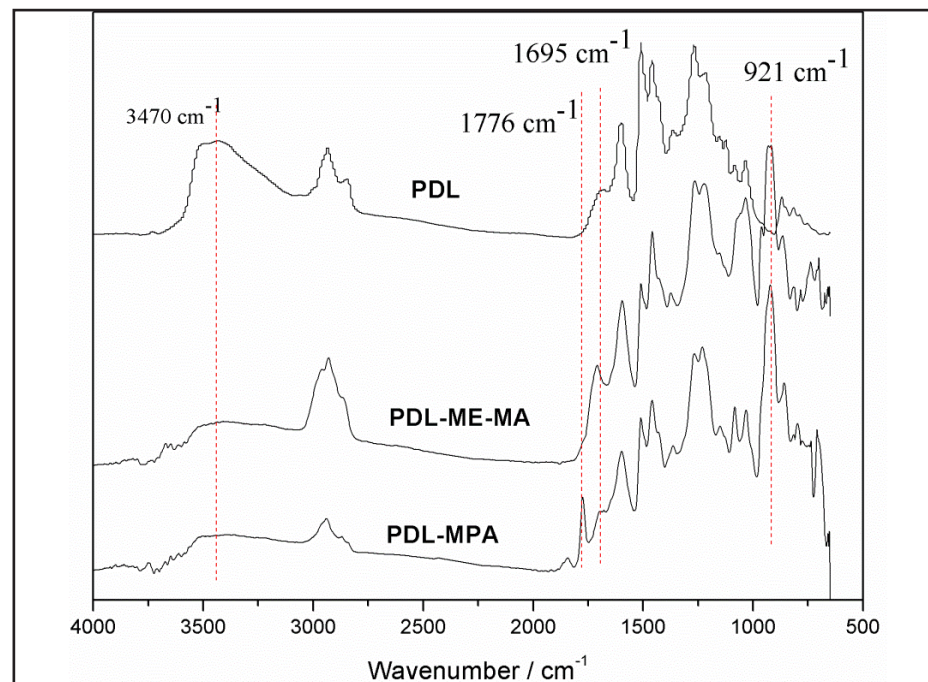


Figure PL-1.17. The FTIR spectra of PDL, PDL-EA-MA and PDL-MPA.

1.6. Application Development of PDL-Based Epoxy Asphalt

Modification of asphalt with PDL-epoxy and EA-MA

We used PDL epoxy system to modify the asphalt for improved performance. Figure PL-1.18 (a) shows the changes of rutting parameter ($G^*/\sin\delta$) with temperature for different PDL-epoxy asphalt compositions. According to the Strategic Highway Research Program (SHRP) tests, the temperature at which $G^*/\sin\delta$ is equal to 1 KPa is defined as the maximum temperature for an asphalt binder to provide effective function in the pavement. As shown in Figure PL-1.18 (a), addition of epoxy as a modifier enhanced the maximum temperature. The neat asphalt exhibited a maximum temperature of $\sim 73^\circ\text{C}$. In contrast, the modified asphalt binders containing 7.5%, 15% and 22.5% PDL-epoxy displayed maximum temperatures of 81°C , 85°C , and 100°C , respectively. This result indicates that PDL-epoxy asphalt binders would provide higher rutting resistance than the neat asphalt binder. The maximum temperature of the 7.5% PDL-epoxy modified asphalt was lower than that of the 7.5% DER332 modified asphalt, which was almost the same as the maximum temperature of the 15% PDL-epoxy asphalt. When the epoxy content was increased to 22.5%, the maximum temperature of the PDL-epoxy asphalt blend was slightly higher than that of the DER 332 asphalt blend. At a 22.5% loading, the superior modification effect of PDL-epoxy over DER332 is probably because the performance of the PDL-epoxy modified asphalt is influenced by two factors, the T_g of the cured epoxy network and its dispersion in the asphalt binder. It is believed that the solid PDL-epoxy was not dispersed as homogeneously as the liquid DER 332. Therefore, at lower concentrations, the better-dispersed DER 332 manifested higher reinforcing effect than PDL-epoxy. However, because PDL-epoxy has a more bulky and rigid structure than DER 332 as discussed above, the cured PDL-epoxy resin exhibits a much higher T_g than the cured DER332. As a consequence, when the epoxy content increased from 15% to 22.5%, the high T_g of PDL-epoxy resin compensated the effect of its poor dispersion in asphalt and could still greatly improve maximum temperature of rutting-resistance.

Figures PL-1.18 (b) and PL-1.18 (c) show the storage and loss moduli for neat asphalt and PDL-epoxy asphalt binders at 60°C . The storage and loss modulus of PDL-epoxy and DER 332 modified asphalts were higher than the neat asphalt and increased with epoxy content. As it was for $G^*/\sin\delta$, the storage and loss moduli of PDL-epoxy modified asphalt were lower than that of DER 332 modified asphalts at low epoxy contents but similar at higher epoxy content. This result suggests that PDL-epoxy resin can impart similar viscoelastic behaviors to asphalt compared to the commercial DER332.

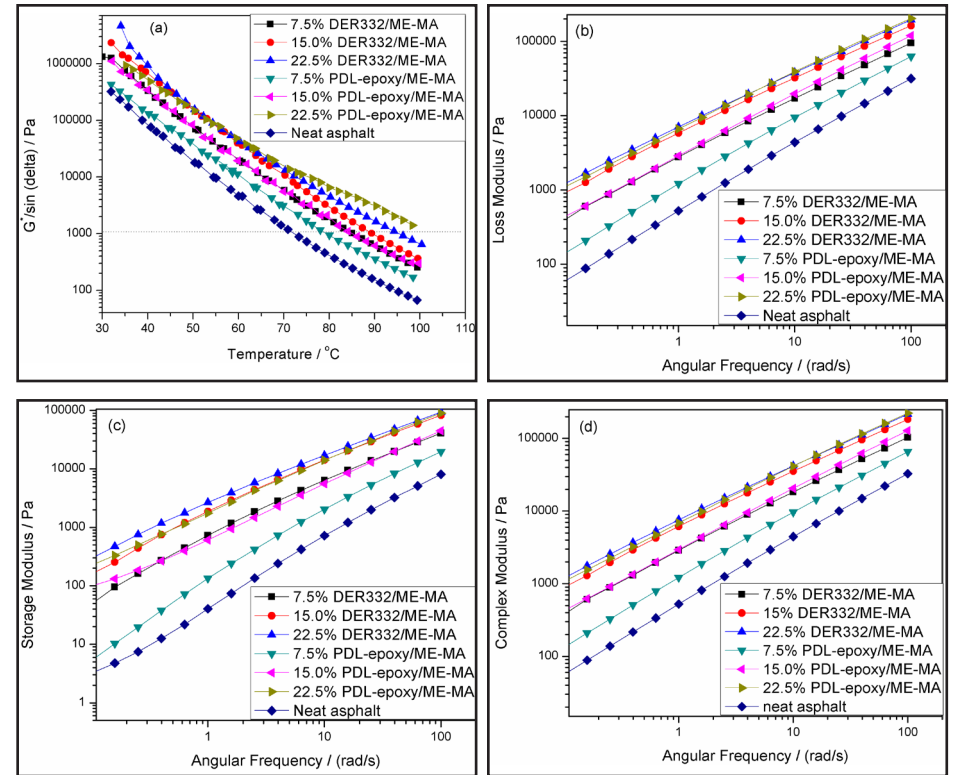


Figure PL-1.18. Effects of epoxy resin contents on the rheological properties of modified asphalt blends by PDL-epoxy and DER332, respectively. (a) Relation of temperature and $G^*/\sin\delta$ at 10 rad/s. At 60°C , effects of frequency on the loss modulus (b), storage modulus (c), and complex modulus (d) of asphalt and epoxy asphalt.

The effect of epoxy resin content on complex modulus (G^*) at 60°C for each binder can be seen in Figure PL-1.18 (d). PDL-epoxy asphalts exhibited higher G^* than the neat asphalt binder in the whole frequency range studied, G^* increased continuously with epoxy resin contents. Also, the PDL-epoxy asphalt displayed similar G^* as the DER 332 epoxy asphalt at 22.5% epoxy content. This result further illustrates that PDL-epoxy will be a potential epoxy modifier for asphalt in place of bisphenol A type epoxy.

Modification of asphalt with PDL based curing agents and DER332

Similarly, rheological tests were also performed on the epoxy asphalt samples with different epoxy content. Figure PL-1.19 (a) shows the plots of rutting parameter ($G^*/\sin\delta$) versus temperature. The addition of epoxy resin as a modifier increased the maximum temperature. Neat asphalt showed a maximum temperature $\sim 73^\circ\text{C}$. In contrast, the modified asphalt binders containing 7.5, 15 and 22.5% displayed maximum temperatures of 84.8, 89, and 100°C for PDL-EA-MA and 90, 96, and $>100^\circ\text{C}$ for PDL-MPA. This result indicates that the rutting resistance of epoxy-asphalt binders was better than the original asphalt binder. In addition, PDL-MPA/DER332 modified asphalts exhibited higher maximum temperatures than corresponding PDL-EA-MA/DER332 modified asphalts. The reason is that MPA has much more rigid structure than EA-MA, giving higher maximum temperature in the resulting epoxy asphalt.

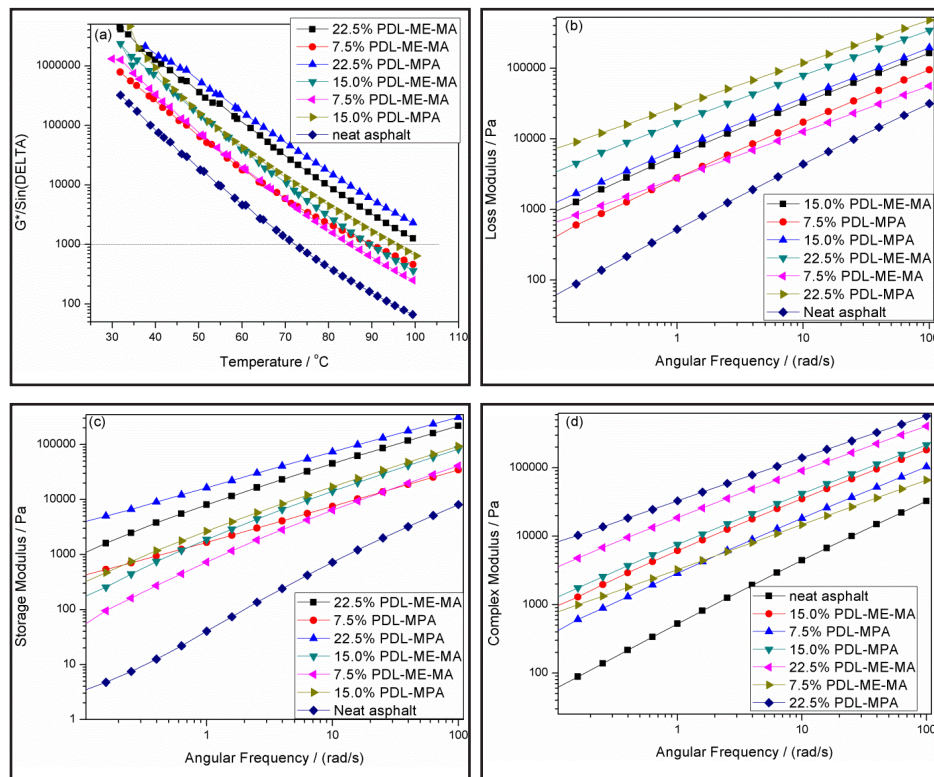


Figure PL-1.19. Effects of epoxy resin contents on the rheological properties of modified asphalt blends by PDL-EA-MA/DER332 and PDL-MPA/DER33, respectively. (a) Relation of temperature and $G^*/\sin\delta$ at 10 rad/s. At 60°C , effects of frequency on the loss modulus (b), storage modulus (c), and complex modulus (d) of asphalt and epoxy asphalt.

Figure PL-1.19 (b, c) show the results of G' and G'' for neat asphalt and epoxy-asphalt binders. G' and G'' of the modified asphalt by DER 332/PDL-curing agents were higher than that of the original asphalt and increased with the content of epoxy resin. Similar to the trend of $G^*/\sin\delta$, the G' and G'' of DER332/PDL-MPA modified asphalt was higher than that of /DER332PDL-EA-MA modified asphalt.

Figure PL-1.19 (d) shows the effect of epoxy resin content on complex modulus (G^*) for each binder. Similarly, epoxy-asphalt presented higher G^* than original asphalt binder. Further, G^* increased with epoxy resin content. Meanwhile, the DER332/PDL-MPA asphalt displayed higher G^* than DER332/PDL-MEMA epoxy asphalt at all epoxy content levels. These results indicate that the epoxy asphalt prepared from PDL based curing agent can greatly improve the performance of asphalt binders.

Conclusion/Discussion

In this task, lignin was successfully converted to epoxy compounds and the lignin-derived epoxy was demonstrated to offer comparable performance as the commercial bisphenol A type epoxy in modifying asphalt. Preparation of Lignin-derived epoxy can be effectively performed by reacting epichlorohydrin (ECH) and partially depolymerized lignin (PDL) at 117°C , resulting in a relatively high yield of the PDL-epoxy product. The thermal and mechanical properties of the PDL-epoxy cured with a Tung oil derived anhydride curing agent (ME-MA) are comparable to that of the bisphenol A type epoxy DER332 cured with the same curing agent. For modification of asphalt, compared to the DER332, the PDL-epoxy asphalt similarly exhibited significant improvement on the viscoelastic performance, especially at elevated temperatures. This study sets up a framework for the modification of asphalt using lignin-derived epoxy, and the results suggest lignin-derived epoxy is promising in epoxy asphalt application.

The PDL-derived polycarboxylic acids were successfully prepared by esterification between PDL and two anhydrides (fatty acid derived anhydride EA-MA and rosin-derived anhydride MPA) with high yields. When used as curing agent for DER332 modified asphalt, PDL-MPA exhibited much better performance in terms of viscoelastic properties of epoxy asphalt than PDL-EA-MA. This study sets up a framework for the modification of asphalt using lignin-derived epoxy, and the results suggest lignin-derived epoxy is promising in epoxy asphalt application.

TASK 2: EXPLORE DEPOLYMERIZATION AND MODIFICATION OF LIGNIN IN SOLID STATE REACTION

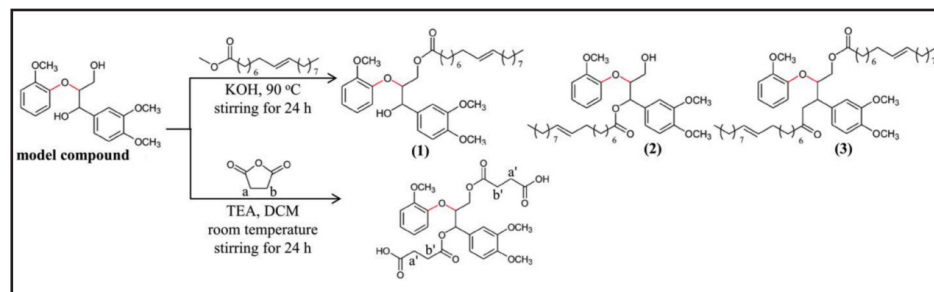
2.1 Simulate esterification of lignin using lignin model compound

Objective

To investigate the bond cleavage and reaction mechanism of lignin modification, the typical dilignol β -O-4 type lignin model compound was prepared and utilized to simulate the esterification reactions of lignin in both solution reaction environments and ball milling process.

Methodology

Scheme PL-2.1 shows the synthetic routines of the esterification reactions of lignin model compound and the likely products. Lignin model compound and potassium hydroxide were dissolved in methyl oleate, the mixture was stirred for 24 h at 90 °C. Lignin model compound, succinic anhydride and triethylamine, were dissolved in dichloromethane and stirred for 24 h at room temperature. These reactions were conducted in ball mill in the absence of solvents as well. The products were purified using gel column. Thin layer chromatography (TLC) and ^1H NMR were used to identify the products and determine the chemical structure.



Scheme PL-2.1. Esterification between lignin model compounds and acylating agents.

Results

Lignin model compound has been synthesized to investigate the bond cleavage of during lignin modification. The dilignol β -O-4 type lignin model compound was prepared because the β -O-4 linkage is the most predominant in lignin structure. In the esterification of lignin model compound with methyl oleate in solution reaction, three new spots were detected by the TLC method, which corresponded to prod-

uct 1, 2 and 3 shown in Scheme PL-2.1. Product 3 was unable to separate from the very nearby methyl oleate and oleic acid during purification process. Figure PL-2.1 exhibits the ^1H NMR spectra of the model compound and the esterified products. Compared to the model compound (Figure PL-2.1a), the spectra of oleated products showed a new peak at 5.3 ppm originated from the two olefinic protons in methyl oleate. For oleated products 1 and 2, the integral ratio of olefinic protons to phenolic protons was 2/7 and the integral ratio of methoxyl protons to phenolic protons is 9/7, which were consistent with their predicted chemical structures. Hence, the transesterification between lignin model compound and methyl oleate was successfully achieved. A trial of this transesterification was also conducted in a ball mill at room temperature, TLC results showed similar products when compared to the ones formed in solution reaction.

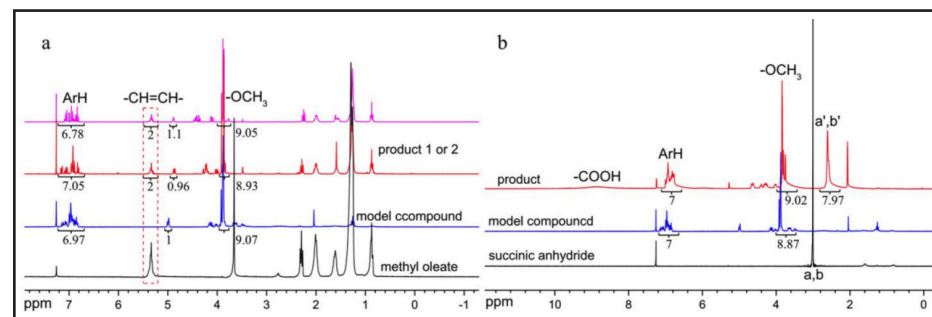


Figure PL-2.1. ^1H -NMR spectra of model compound with (a) oleated products and (b) succinate product through solution reactions.

The esterification between model compound A and succinic anhydride is shown in Scheme PL-2.1. In the ^1H NMR spectrum of the succinate product (Figure PL-2.1b), the peak at 2.6 ppm was assigned to the identical methylenic groups in the butanedioic monoester originated from succinic anhydride. The integral ratio of methoxyl protons to phenolic protons was 9/7 for succinate monoester product, which was in agreement with the model compound. In addition, the integral ratio of methylenic protons from the butanedioic monoester to phenolic protons was 8/7, which was consistent with the predicted chemical structure of succinate product. The hump at ~9 ppm corresponded to the carboxylic acid groups in product. The formation of a new peak at 2.6 ppm of methylenic groups indicated successful occurring of the esterification between the hydroxyls of model compound and succinic anhydride. Correspondingly, the same esterification was performed in a ball mill without using solvents, and the succinate product appeared after 30 min of milling. As shown in Figure PL-2.2, the succinate product showed a distinct peak

at 2.6 ppm attributed to methylenic groups when compared with lignin model compound. The reaction results in ball milling process are in agreement with the results through solution reactions.

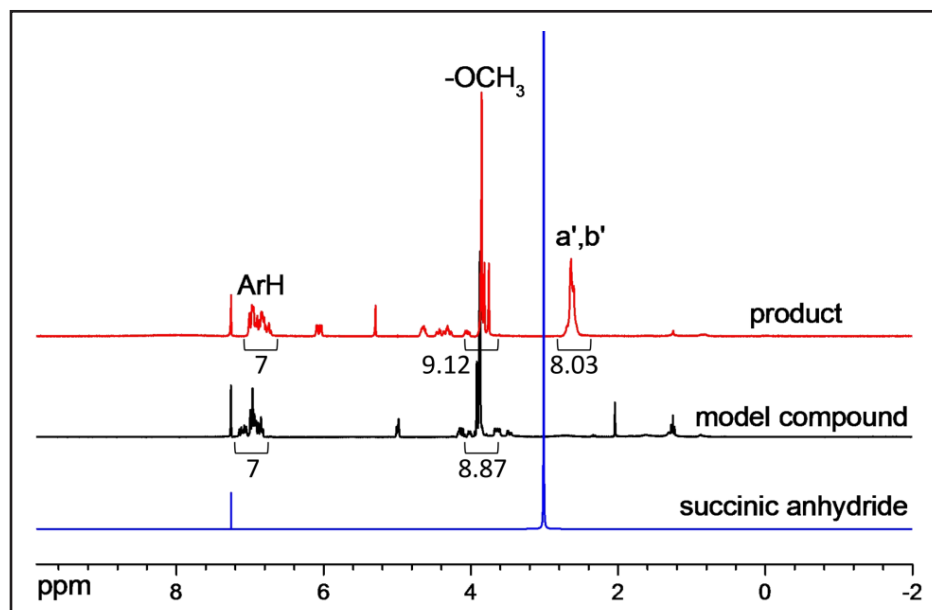


Figure PL-2.2. ¹H-NMR spectra of model compound with succinate product through ball milling.

Conclusion/Discussion

The simulation of esterification of lignin was performed using a lignin model compound. The esterifications between lignin model compound and acylating agents were successfully achieved in both solution and ball milling process. This study demonstrates that mechanical force activated reaction, such as reaction in ball milling, can be used to modify the structure of lignin, and is more economically and environmentally friendly.

2.2. Oleation of lignin via ball milling and its application in thermoplastic materials

Objective

Although the aliphatic and aromatic hydroxyls of lignin are chemically reactive, the high molecular weight and highly branched structure of lignin make it not soluble in most solvents and the hydroxyls less accessible to the chemical reagents for reactions. Ball milling is a common mechanical treatment to diminish the lignin particle size and increase the accessibility to reagents. Some researches indicate that the

mechanical energy generated during ball milling process initiate structural change and bond cleavage in lignin. In this study, lignin and methyl oleate were ground in a ball mill in the presence of KOH to achieve oleated lignin. Subsequently, the oleated lignin was blended with PLA and effect of chemical modification on the compatibility between lignin and PLA was studied.

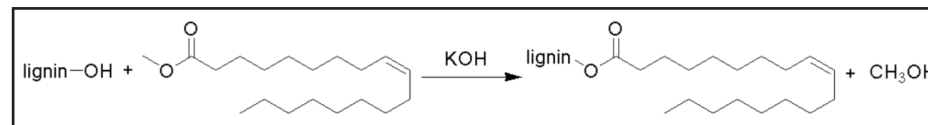
Methodology

The transesterification was carried out in a planetary ball mill (PQ-N04 Gear Drive 4-Station) under room temperature. Lignin, methyl oleate and potassium hydroxide were mixed and milled in a 100 mL zirconia jar. The chemical structure was examined using ¹H NMR and FT-IR. The milling time was 90 min with an alternative cycle of 15 min at 50 Hz under the bidirectional mode. PLA and lignin (w/w = 90/10 or 70/30) were compounded using micro conical twin-screw compounder (HAAKE Minilab II). The screw speed was set at 100 rpm for all runs, and the extrusion temperature was 180 °C. Test specimens were prepared by a Minijet (HAAKE MiniJet II). Prior to testing, all specimens were conditioned at 23 °C and 50% RH for one week. Morphological structures, mechanical and thermomechanical properties of the PLA/lignin blends were studied.

Results

Oleation of lignin via mechanochemical transesterification

The transesterification between lignin and methyl oleate was performed in the presence of KOH through mechanically grinding in a ball mill. The schematic of this transesterification is illustrated in Scheme PL-2.2. The breakup of intra- and inter-molecular hydrogen bonds and cleaving of the β-O-4 linkages are mechanochemically activated during milling process. These hydroxyl groups of lignin reacted with methyl oleate to establish new ester bonds.



Scheme PL-2.2. Transesterification between lignin and methyl oleate.

Figure PL-2.3 shows the FT-IR spectra of NARA lignin and oleated lignin. Compared to the unmodified NARA lignin, the oleated NARA lignin displayed a peak at 1720 cm⁻¹ attributed to the stretching carbonyls of ester bond. In addition, the peak intensity of the carbonyls at 1720 cm⁻¹ for LMO milled with Na₂SO₄ is much higher than that of LMO milled without Na₂SO₄, which indicates that the addition of milling medium improves the reaction conversion and efficiency. The peak at ~3400 cm⁻¹ corresponds to the stretching vibration of O-H, and the peaks at ~1600 cm⁻¹ and ~1500 cm⁻¹ was attributed to the stretching of the double bonds of the aromatic rings [Yang, H. et al., 2007; Pandey, 1999].

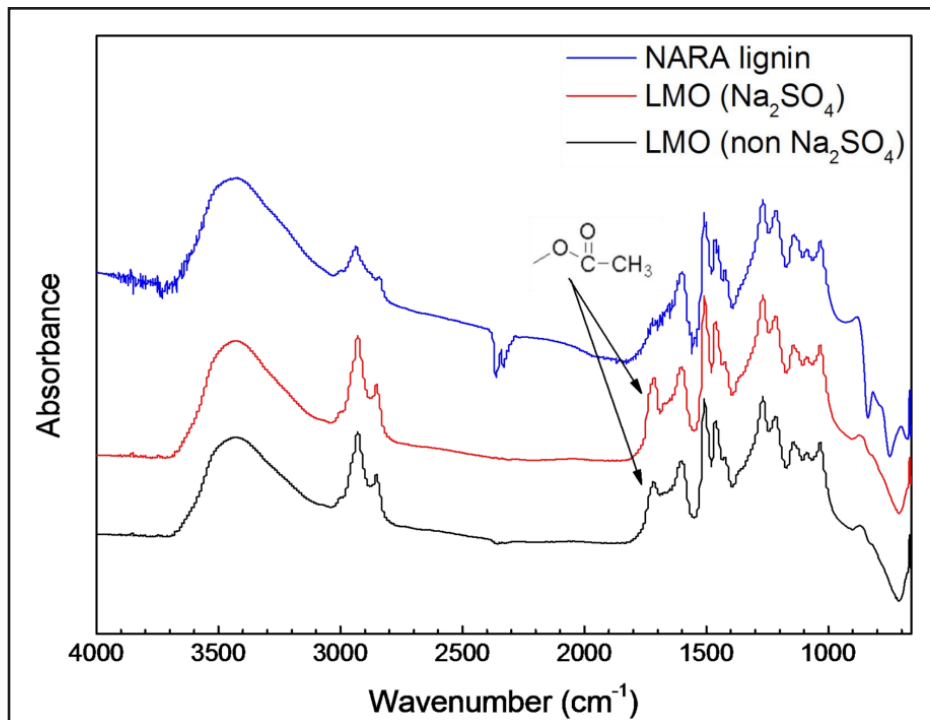


Figure PL-2.3. FT-IR spectra of NARA lignin and oleated lignin w/ and w/o milling medium. LMO: lignin modified by methyl oleate.

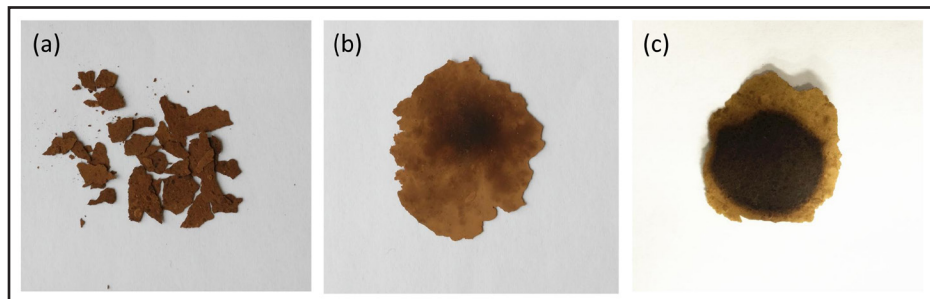


Figure PL-2.4. Images of hot pressed samples for (a) NARA (wood milled) lignin and (b) LMO (no Na_2SO_4) at 200 °C, and for (c) LMO (Na_2SO_4) at 150 °C. LMO: lignin modified by methyl oleate.

Hot pressing tests were performed to examine the thermoplasticity of lignin before and after mechanochemical modification as shown in Figure PL-2.4. The unmodified lignin and LMO (non Na_2SO_4) were compressed under 200 °C, but LMO (Na_2SO_4) was compressed under 150 °C because it became very fluid at 200 °C. The unmodified lignin shattered into pieces after demolding (Figure PL-2.4a), while LMO formed a homogeneous thin film (Figure PL-2.4b). This result demonstrated that

the thermoplasticity of lignin was improved greatly after mechanically activated transesterification. It is also noted that the modified lignin using Na_2SO_4 as milling medium exhibited better thermoplasticity and processability (Figure PL-2.4c vs. Figure PL-2.4a).

The dynamic mechanical properties of unmodified and oleated lignin powder were measured using a foldable aluminum mold. Figure PL-2.5 shows the curves of tan delta versus temperature for the unmodified lignin and LMO (Na_2SO_4). Lignins exhibited a T_g around 80 °C before and after the mechanochemical oleation. The T_g of LMO slightly decreased from 80.2 °C of NARA lignin to 77.8 °C. The fatty acid chains introduced into LMO acted as soft segments, which led to a mild decline of the T_g .

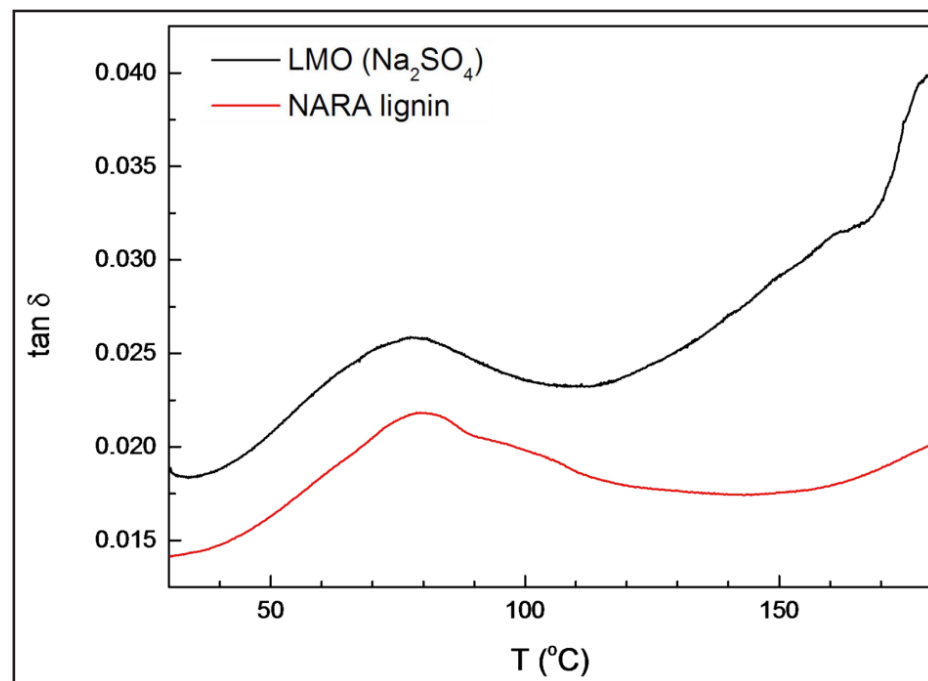


Figure PL-2.5. DMA curves of tan delta versus temperature of unmodified and oleated lignin. LMO: lignin modified by methyl oleate.

2.3 Blending of PLA and oleated lignin and properties of the blends

PLA/lignin blends were prepared through melt extrusion at 185 °C. Figure PL-2.6 shows the extruded samples and injection molded bars, and Figure PL-2.7 shows the SEM micrographs of PLA/lignin blends. The flattened surfaces of the PLA/lignin blends were cut using a microtome at room temperature. By comparing Figures PL-2.7 (a) and (b), it is noted that the size of dispersed lignin particles decreased significantly after mechanically activated transesterification between lignin and methyl oleate. Moreover, Figure PL-2.7 (c) exhibited a finer dispersion and smaller particle size of lignin particles when compared to Figure PL-2.7 (b), which indicates that the addition of milling medium during grinding process improved the interfacial adhesion between PLA and lignin.

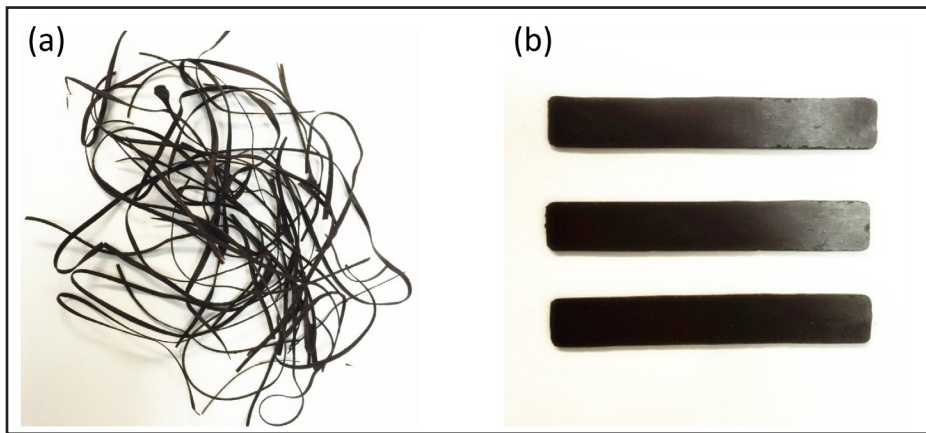


Figure PL-2.6. Photos of (a) extrudate of PLA/lignin (70/30 w/w) blends through melt extrusion and (b) sample bars of PLA/lignin (70/30 w/w) blends through injection molding.

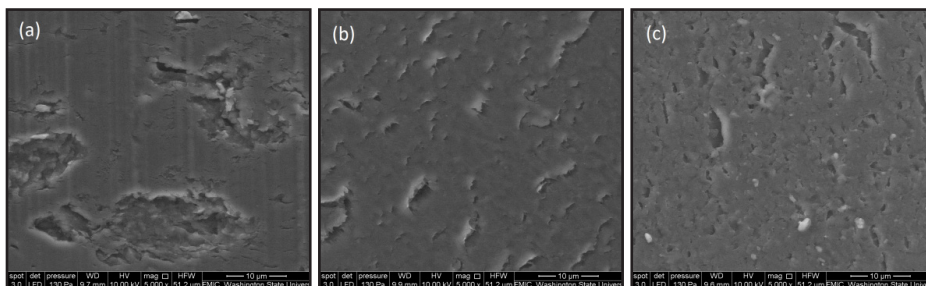


Figure PL-2.7. SEM images of flat-cut surfaces for (a) PLA/NARA lignin blends, (b) PLA/LMO (non Na_2SO_4) blends and (c) PLA/LMO (Na_2SO_4) blends. (PLA/lignin = 70/30 (w/w)).

To determine thermal properties, the sample was first heated to 200°C at 10 °C / min and then held isothermally for 2 min to erase the thermal history. Next, the sample was cooled to 0°C at 10 °C/min, and was finally heated to 200 °C at the same rate. As shown in Figure PL-2.8, the glass transition temperature (T_g) of neat PLA is higher than that of PLA/lignin blends, especially for oleated lignin. The significant reduction in T_g of PLA/LMO blends is probably due to the addition of oleated lignin since the attached long aliphatic chain is likely to plasticize PLA. In addition, the T_g of PLA/LMO blends (Na_2SO_4) displayed lower T_g than PLA/LMO blends (non Na_2SO_4). This suggests that the addition of Na_2SO_4 as a milling medium improved the conversion of oleation of lignin during ball milling process, which resulted in enhanced plasticizing effect and lower T_g for PLA/LMO blends (Na_2SO_4). From Figure PL-2.8b, the cold crystallization temperature (T_{cc}) of PLA/LMO blends was lower than neat PLA and its blends with unmodified lignin, indicating that oleated lignin improved the ability of crystallization for PLA than unmodified lignin. The values of T_g and T_{cc} for the PLA/lignin blends were listed in Table PL-2.1.

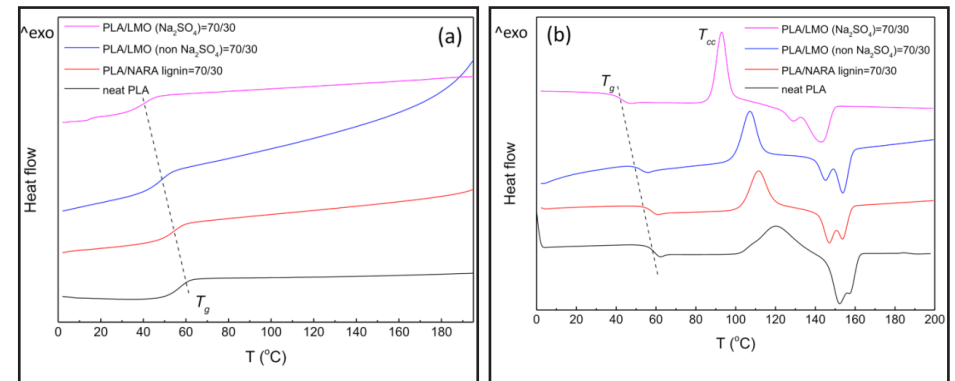


Figure PL-2.8. DSC curves of PLA/lignin blends: (a) first cooling and (b) second heating.

Table PL-2.1. Thermal properties of the PLA and lignin blends.

Sample	T_g (°C)	T_{cc} (°C)
neat PLA	58.0	120
PLA/NARA lignin=70/30	57.2	111
PLA/LMO (non Na_2SO_4)=70/30	52.5	107.5
PLA/LMO (Na_2SO_4)=70/30	42.7	93.3

Table PL-2.2 lists the tensile properties of the PLA/lignin blends. All samples displayed brittle fracture behaviors. The modulus of neat PLA was higher than that of the PLA/lignin blends. In addition, the PLA/oleated NL blends showed slightly

higher modulus than the PLA/NL blends, which was mainly attributed to the better compatibility between PLA and oleated NL. The improved compatibility between two phases presented strong effect on the tensile strength as the PLA/oleated NL blends showed significantly higher strength than the PLA/NL at the same lignin weight content. Meanwhile, the addition of lignin at these levels in PLA caused a significant decline on the tensile strength when compared with neat PLA. With increasing the lignin content in PLA, the elongation at break of PLA/lignin blends decreased. Moreover, the PLA/oleatedNL blends showed slightly higher elongation at break than the PLA/NL blends due to the improved compatibility.

Table PL-2.2. Mechanical properties of the PLA/lignin blends.

sample	Elastic modulus	Tensile strength	Elongation@break
	GPa	MPa	%
neat PLA	3.31±0.23	57.03±1.37	3.45±0.03
oleatedNL10*	3.14±0.40	51.57±0.93	3.25±0.27
NL10	2.95±0.31	45.23±1.40	2.95±0.17
oleatedNL30	2.89±0.20	42.17±2.36	2.90±0.06
NL30	2.74±0.42	38.07±2.50	2.55±0.20

*OleatedNL: LMO (Na₂SO₄); NL: unmodified lignin; 10 and 30: 10 and 30 wt% lignin content in PLA/lignin blends.

Conclusion/Discussion

The mechanically activated transesterification was successfully carried out between NARA (wood milled) lignin and methyl oleate through grinding in a ball mill. The effect of milling medium (Na₂SO₄) on the reaction was also explored as lignin and methyl oleate were milled with and, respectively. FT-IR results indicate that the use of milling medium improved the efficiency and conversion of transesterification. After reacted with methyl oleate, the thermoplasticity was greatly improved. PLA/LMO blends exhibited a finer and homogeneous dispersion of lignin particles than PLA/NARA lignin blends. Milling with Na₂SO₄ resulted LMO having improved compatibility with PLA as the PLA blends with the former displayed lower T_g than PLA blends with the latter. This result was probably because the addition of Na₂SO₄ as milling media improved the conversion of oleation of lignin and hence enhanced plasticizing effect for PLA. T_g of neat PLA is much higher than that of PLA/oleated NARA lignin blends, indicating the attached long aliphatic chain in lignin is likely to plasticize PLA. The PLA/oleated NL blends presented finer dispersion in PLA and smaller particle size of lignin particles compared to the PLA/NL blends and exhibited higher tensile modulus and strength of PLA/oleated NL blends.

2.4. Esterification of lignin using various anhydrides through ball milling and its application in thermosetting materials

Objective

From the section (2.2), we know that the certain amount of hydroxyl groups present in lignin can be effectively functionalized via mechanically activated grinding. In this section (2.4), we prepared lignin based polycarboxylic acids (LPCA) through mechanochemical esterification with various anhydrides. The esterification reactions between NARA lignin and two cyclic anhydrides were investigated in the ball milling process. The LPCAs were used as curing agents for a commercial epoxy resin (DER353).

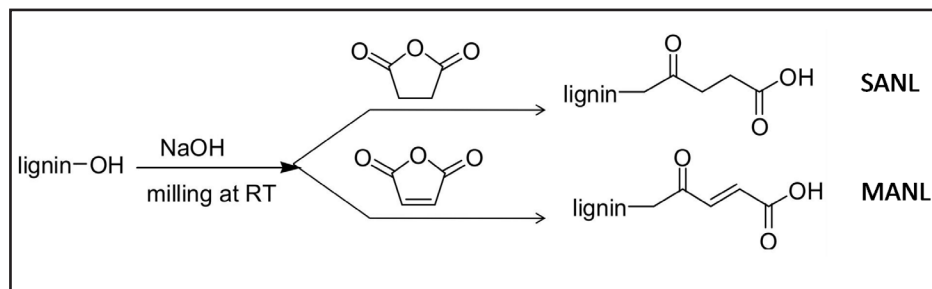
Methodology

The esterification was carried out at room temperature in a planetary ball mill (PQ-N04 Gear Drive 4-Station). Lignin, anhydride, and base were milled in a zirconia jar. The milling time was 90 min with an alternative cycle of 15 min at 50 Hz under the bidirectional mode. The resulting LPCA was then used as curing agent or co-curing agent for DER 353. When used a co-curing agent, LPCA was used together with nadic methyl anhydride (NMA) for the curing of the epoxy. 1 wt% 2-ethyl-4-methylimidazole (EMID) was added as a catalyst.

Results

Based on the results from the model compound, NARA lignin was reacted with anhydride to prepare lignin-based polycarboxylic acids and the products were subsequently used as curing agents for a commercial epoxy. The schematic reactions of alkali-catalyzed esterification of NARA lignin with two anhydrides are shown in Scheme PL-2.3. Succinic anhydride and maleic anhydride were chosen to react with NARA lignin through mechanically milling to form lignin-based polycarboxylic acids. The mechanochemical modification of NARA lignin was performed at an anhydride to lignin mass ratio of 1.2:1 with 5 wt% NaOH as catalyst on the basis of total reactant weight. The hydroxyls of lignin reacted with anhydride to form lignin-based monoester under alkaline condition during ball milling process. As shown in Figure PL-2.9a, a distinct peak at 1730 cm⁻¹ attributed to the carbonyl groups is noted in the FTIR spectrum of SANL (esterified NARA lignin with succinic anhydride) when compared with the unmodified NARA lignin. Similarly, a peak at 1726 cm⁻¹ is also noted in the FTIR spectrum of MANL (esterified NARA lignin with maleic anhydride Figure PL-2.9b). Generally, the carbonyl groups of monoester exhibit an absorption peak at ~1730 cm⁻¹, and the carbonyl groups of carboxylic acid gives an absorption peak at 1712 cm⁻¹. In this case, these peaks were overlapped to result in a peak

centered at $\sim 1730\text{ cm}^{-1}$ [Xiao et al. 2001; Thielemans & Wool, 2005]. This result indicates the lignin-based polycarboxylic acids were successfully prepared through mechanochemically activated esterification between lignin and anhydrides during ball milling process.



Scheme PL-2.3. Esterification of lignin using succinic anhydride and maleic anhydride.

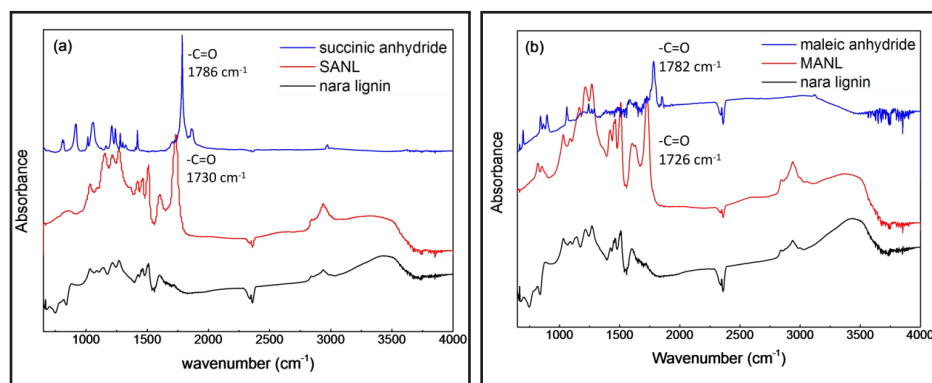
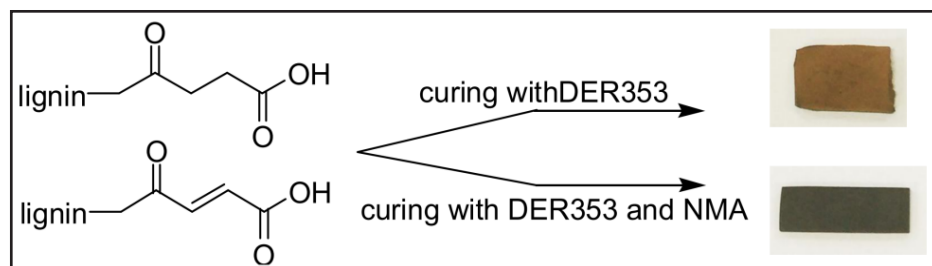


Figure PL-2.9. FT-IR spectra of unmodified and esterified nara lignins with: (a) succinic anhydride and (b) maleic anhydride.

Lignin-based carboxylic acids (LPCAs) prepared can be used for curing of epoxies alone or in combination with other co-curing agent (Scheme PL-2.4). Because of its relatively high molecular weight and solid form, LPCA does not mix very well with DER353. Using a liquid co-curing agent helps to improve the curing efficiency



Scheme PL-2.4. Schematic routine of preparing cured lignin-based epoxy resin.

and compatibility of LPCAs and DER353. The co-curing also reduces the viscosity of the LPCA/DER353 resin system, resulting in better processability and properties of lignin-based cured resins.

As mentioned previously, NMA was chosen as a co-curing agent in combination with LPCA for the curing of DER353. Non-isothermal curing kinetics was studied by DSC at heating rates of 2.5, 5, 7.5, 10 and 12.5 °C/min, respectively. The resin system was composed of DER353 (epoxy resin), SANL/MANL (curing agent) and NMA (co-curing agent) in a ratio of 1.5:1:0.8 (w/w/w). As shown in Figure PL-2.10, curing of the tricomponent resin systems (LPAC-NMA-DER35) showed only one major exothermal peak attributed to the major curing reaction of carboxyls and epoxides. With increasing the heating rate, the exothermal peak temperature shifted to higher temperature. The curing kinetics was studied using Ozawa method to calculate the activation energy (E_a). Ozawa's equation is expressed as follows:

$$E_a = -\frac{R}{1.052} \times \frac{d \ln \varphi}{d(1/T_p)} \quad (1)$$

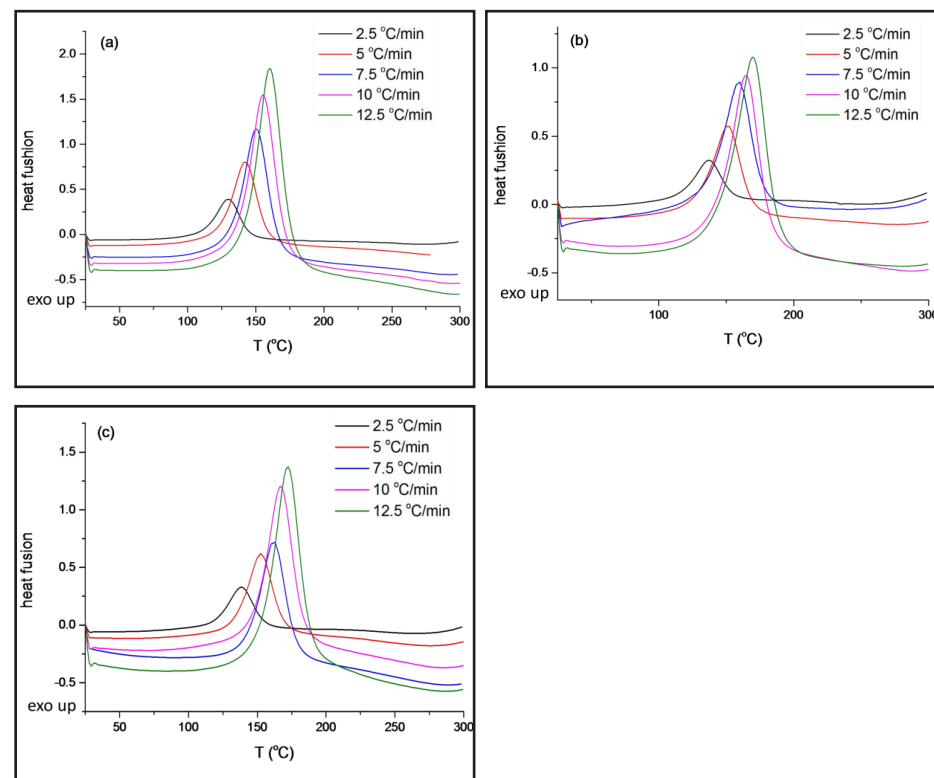


Figure PL-2.10. DSC exotherms of curing processes of tricomponent resin systems at heating rates of 2.5, 5, 7.5, 10 and 12.5 °C/min: (a) NMA-DER353, (b) SANL-NMA-DER353 and (c) MANL-NMA-DER353.

Where E_a is the activation energy, R the ideal gas content, ϕ the heating rate and T_p the peak temperature. Therefore, E_a can be determined from the slope of $\ln\phi$ against $1/T_p$ of Ozawa plot (Figure PL-2.11).

The activation energy of NMA-DER353 and LPCA/NMA/DER353 resin systems are summarized in Table PL-2.3.

According to Equation 1, activation energy (E_a) calculated through Ozawa method was 76.46, 69.47 and 70.37 KJ/mol for NMA-DER353, SANL-NMA-DER353 and MANL-NMA-DER353 resin systems, respectively. It is obvious that the E_a of NMA-DER353 resin system is much higher than that of LPCAs-NMA-DER353 resin system. This result suggests that the addition of LPCAs in resin system improves the reactivity of curing reaction with epoxides.

Table PL-2.3. Activation energy (E_a) and glass transition temperature (T_g).

Sample	E_a (KJ/mol)	T_g (°C)
NMA-DER353	76.5	144.0
SANL-NMA-DER353	69.6	134.8
MANL-NMA-DER353	70.4	139.3

The thermal mechanical properties of DER353 cured with NMA and LPCA-NMA were evaluated though DMA and shown in Figure PL-2.12. Figure PL-2.12a shows that the storage moduli of cure NMA-DER353 and LPCA-NMA-DER353 are comparable among glassy state, which means the addition of LPCA as curing agent won't sacrifice the stiffness of cured epoxy resin. As shown in Figure PL-2.12c, the glass transition temperature (T_g) of cured NMA-DER353 resin exhibited the T_g of 144.53 °C, which was about 10 °C higher than that of cured LPCA-NMA-DER353 resin. This result indicates that NMA possessed a more rigid molecular structure than LPCAs. In addition, the T_g of SANL-NMA-DER353 is lower than that of MANL-NMA-DER353, which exhibited that the introduced succinate monoester in NARA lignin made the molecular chains of esterified NARA lignin more flexible than the introduced maleate monoester.

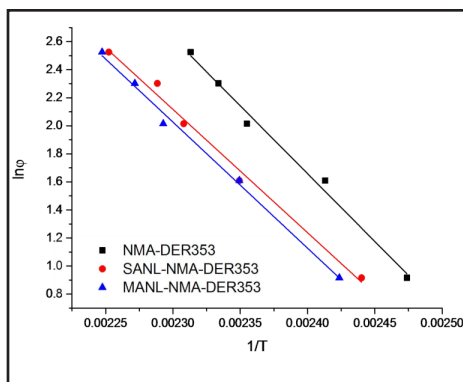


Figure PL-2.11. Plot of $\ln\phi$ versus $1/T_p$ by Qzawa method: (a) NMA-DER353, (b) SANL-NMA-DER353 and (c) MANL-NMA-DER353.

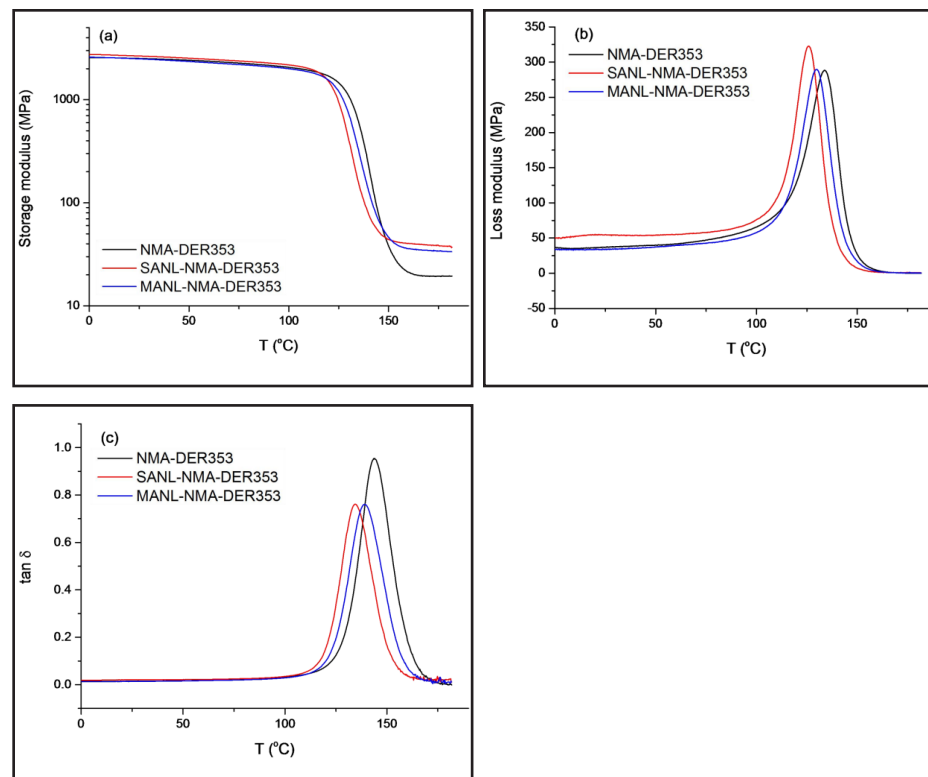


Figure PL-2.12. Storage modulus (a), loss modulus (b) and tan delta (c) of cured LPCA-NMA-DER353 versus temperature.

Thermal stability of cured LPCA-NMA-DER353 resins was examined by TGA. Figure PL-2.13 shows the decomposition behaviors of cured NMA-DER353 and LPCA-NMA-DER353 resins. The cured NMA-DER353 resins displayed a very similar degradation temperature to that of the cured LPCA-NMA-DER353 resins (the degradation temperatures at 5 % weight loss are 300.1, 298.5 and 296.0 for NMA-DER353, MANL-NMA-DER353 and SANL-NMA-DER353, respectively), meaning that replacing part of NMA by LPCA exhibited little influence on degradation behavior. However, both cured samples with lignin-derived curing agents exhibited higher thermal stability as it was reflected in the higher char residues. This result was probably attributed to the aromatic nature of the LPCA curing agents.

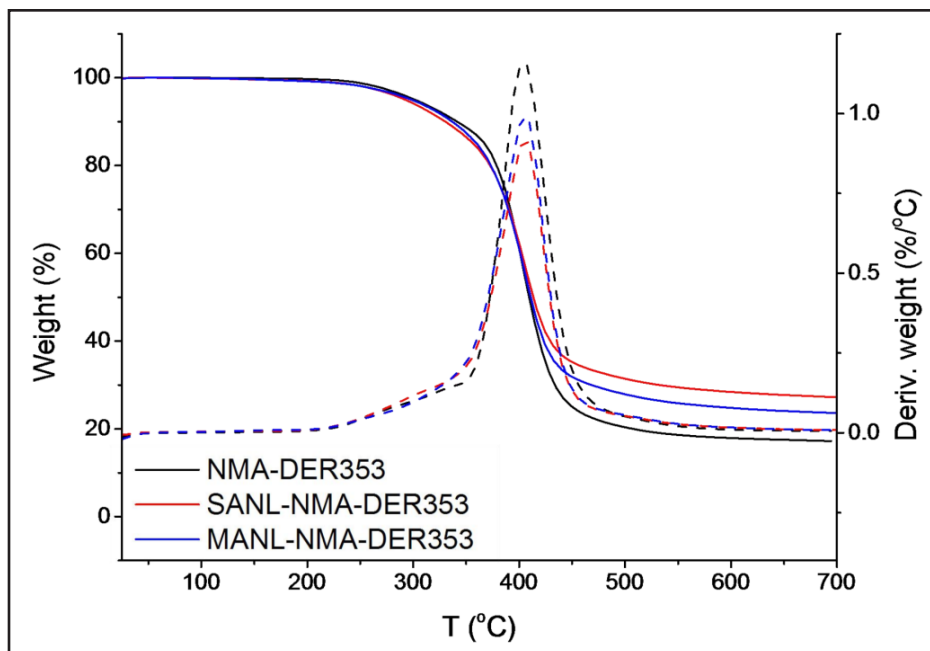


Figure PL-2.13. TGA curves of cured LPCA-NMA-DER353 resins.

Conclusion/Discussion

Lignin-based polycarboxylic acids (LPCAs) were successfully prepared through mechanochemical esterification with anhydrides by ball milling. For the esterification between lignin and succinic anhydride during ball milling process, the absorption peak at 1733 cm^{-1} corresponds to the carbonyl bonds in monoester and carboxylic acid of lignin, indicating that the hydroxyls of lignin have reacted with succinic anhydride to form lignin-based polycarboxylic acids. Curing of DER353 with LPCA and co-curing agent was studied and modeled using the Ozawa method. The lower activation energy of LPCA-NMA-DER353 than NMA-DER353 indicates the addition of LPCAs improves the reactivity of curing. DMA results showed that the cured LPCA-NMA-DER353 had lower T_g than cured NMA-DER353, which was probably due to the higher crosslink density resulted from curing with NMA. The thermal stability of formed char at high temperature region was obviously improved for the epoxy resin cured with LPCAs.

NARA OUTPUTS

Conference Proceedings and Abstracts from Professional Meetings

1. Jianglei Qin, Michael P. Wolcott, Jinwen Zhang. 2012. Diversifying renewable feedstocks for new biobased polymers and applications, Oral presentation at 2012BioEnvironmentalPolymer SocietyMeeting in Denton, Texas, Sept.18-21,2012.
2. Jianglei Qin, Michael P. Wolcott, Jinwen Zhang. 2012. Use of lignin as feedstock for polymer materials: epoxies and curing agents. Poster presentation at NARA 2012 Annual Meeting, Missoula, MT, Sept 13-14, 2012.
3. Jianglei Qin, Junna Xin, Michael P. Wolcott and J. Zhang. 2013. Use of Lignin as Feedstock for Epoxy Application, at 2013 International Wood Composite Symposium, Seattle, WA, April. 3- 4.
4. Jinwen Zhang. 2013. Diversifying Biobased Polymers and Expanding the Window of Properties via Manipulating the Structures of Building Blocks, First International Biobased Macromolecule Material Forum, Nov 13 – 14, NingBo, China (invited)
5. Junna Xin, Jianglei Qin, Daniel Leong, Michael P. Wolcott, and Jinwen Zhang. Exploration of lignin partial depolymerization and development of polymer materials applications. Poster presentation at the NARA Annual Meeting, Corvallis, OR, September 10, 2013.
6. Jinwen Zhang. 2014. Improving the performance of biobased polymers via manipulating the structures of building blocks, the 13th International Symposium on Bioplastics, Biocomposites and Biorefining, May 19 – 24, 2014, Guelph, Ontario, Canada. (invited)
7. Junna Xin, Michael P. Wolcott, Jinwen Zhang, 2014, Partially depolymerized enzymolysis lignin: preparation, characterization and application. Poster presentation at NARA 2014 Annual Meeting, Seattle, WA, Sept. 15-17.
8. Junna Xin, Xiaojie Guo, JinwenZhang, 2015, Application development of lignin: thermosets and polymer blends. Poster presentation at NARA 2015 Annual Meeting, Spokane, WA, Sept. 15-17.
9. Junna Xin, Xiaojie Guo, Jinwen Zhang*, Performance enhancement of lignin-based thermosets and polymer blends, Pacificchem 2015, Honolulu, Hawaii, USA, 2015, Dec 15-20 (oral presentation).
10. Xiaojie Guo, Jinwen Zhang, Junna Xin, Mechanochemical modification of lignin and application of the modified lignin for thermoplastics and thermosets, APS (the American Physical Society) meeting 2016, Baltimore, Maryland, USA, March 14-18. (oral presentation).
11. Jinwen Zhang. **Keynote lecture:** Broadening the Properties and Application Windows of Biobased Polymers, 14th International Symposium on Bioplastics, Biocomposites & Biorefining, May 31 – June 3, 2016, Guelph, Canada.

12. Jinwen Zhang. Broadening the Property and Application Windows of Biobased Polymers by Diversifying Building Blocks, 2015 Pacific Polymer Conference, Kauai, HI, December 9 - 13, 2015.
13. Jinwen Zhang. Performance enhancement of lignin-based thermosets and polymer blends, 2015 Metabolic Engineering and Green Manufacturing in Microorganisms, July 8 -11, 2015, Beijing, China.

Publications

1. Jianglei Qin, Hongzhi Liu, Pei Zhang, Michael P. Wolcott and Jinwen Zhang, Use of eugenol and rosin as feedstocks for biobased epoxy resins and study of curing and performance properties. *Polymer International*, 2014, 63:760-765.
2. Jianglei Qin, Michael Wolcott, Jinwen Zhang, Use of polycarboxylic acid derived from partially depolymerized lignin as a curing agent for epoxy application, *ACS Sustainable Chemistry & Engineering*, 2014, 2:188-193.
3. Junna Xin, Pei Zhang, Michael P. Wolcott, Xiao Zhang, Jinwen Zhang, Partial depolymerization of enzymolysis lignin via mild hydrogenolysis over Raney Nickel. *Bioresource Technology*, 2014, 155:422-426.
4. Junna Xin, Mei Li, Ran Li, Michael P. Wolcott, Jinwen Zhang. A green epoxy resin system based on lignin and tung oil and its application in epoxy asphalt, *ACS Sustainable Chemistry & Engineering*, 2016, 4(5): 2754-2761.
5. Xiaojie Guo, Xin Junna, Michael P. Wolcott, Jinwen Zhang. Mechanochemical synthesis of oleated lignin and properties of its blends with PLA, 2016, *ChemistrySelect*, DOI: 10.1002/slct.201600633.
6. Junna Xin; Pei Zhang; Jinwen Zhang. A novel and formaldehyde-free preparation method for lignin amine and its enhancement for soy protein adhesive, *Journal of Polymers and the Environment*, 2016, under review.
7. Xiaoxu Teng, Hui Xu, Jianwei Shi, Junna Xin, Jinwen Zhang, Preparation and characterization of a new hydrogel via lignosulfonate amine, *ACS Sustainable Chemistry & Engineering*, 2016, under review

Thesis and Dissertations

Xiaojie Guo, PhD Thesis: Investigation of mechanochemical modification of lignin through one-step and solvent-free ball milling, Washington State University, (7/2017, expected)

NARA OUTCOMES

We are looking for the cooperation with industry to implement some of the technologies developed from this work. At this point, there is no contract with any industry partner.

FUTURE DEVELOPMENT

Based on our preliminary result, we will continue to investigate the potential application for lignin based epoxy in asphalt binder as well as the novel hydrogel material prepared from the crosslinked copolymer of lignosulfonate in fertilizer releasing. On the other hand, a new type of smart hydrogel based on lignin will be developed. This special hydrogel is featured by thermo-responsive to temperature and will be explored to effectively remove the metallic ions that existed in industrial wastewater.

LIST OF REFERENCES

- Cateto, C.A., Barreiro, M.F., Rodrigues, A.E. & Belgacem, M.N. (2009). Optimization study of lignin oxypropylation in view of the preparation of polyurethane rigid foams. *Industrial & Engineering Chemistry Research*, 48(5), 2583-2589.
- Chen, W., Liu, X., Dai, P., Chen, Y. & Jiang, Z. (2012). Preparation and mechanical properties of lignin/epoxy resin composites. *Advanced Materials Research*, 482-484, 1959-1962.
- Cong, P., Yu, J. & Chen, S. (2010). Effects of epoxy resin contents on the rheological properties of epoxy-asphalt blends. *Journal of applied polymer science*, 118 (6), 3678-3684.
- Hofmann, K. & Glasser, W. (1994) Engineering plastics from lignin, 23. Network formation of lignin based epoxy resins. *Macromolecular Chemistry and Physics*, 195, 65-80.
- Li, Y. & Ragauskas, A. J. (2012a). Kraft lignin-based rigid polyurethane foam. *Journal of Wood Chemistry and Technology*, 32 (3), 210-224.
- Li, Y. & Ragauskas, A. J. (2012b). Ethanol organosolv lignin-based rigid polyurethane foam reinforced with cellulose nanowhiskers. *Rsc Advances*, 2 (8), 3347-3351.
- Li, Y. & Sarkanen, S. (2002). Alkylated kraft lignin-based thermoplastic blends with aliphatic polyesters. *Macromolecules*, 35(26), 9707-9715.
- Li, Y. & Sarkanen, S. (2005). Miscible blends of kraft lignin derivatives with low-Tg polymers. *Macromolecules*, 38(6), 2296-2306.
- Liu, X., Xin, W. & Zhang, J. (2009). Rosin-based acid anhydrides as alternatives to petrochemical curing agents. *Green Chemistry*, 11, 1018-1025.
- Liu, Z., Zong, L., Zhao, L. & Xie, X. (2013). Preparation and storage stability of asphalt emulsions made from modified lignin cationic asphalt emulsifiers. *Applied Mechanics and Materials*, 357-360, 781-785.
- Mansouri, N.E.E., Yuan, Q. & Huang, F. (2011). Characterization of alkaline lignins for use in phenol-formaldehyde and epoxy resins. *BioResources*, 6(3), 2647-2662.
- Miller, J.E., Evans, L., Littlewolf, A. & Trudell, D.E. (1999). Batch microreactor studies of lignin and lignin model compound depolymerization by bases in alcohol solvents. *Fuel*, 78(11), 1363-1366.
- Pandey, M.P. & Kim, C.S. (2011). Lignin depolymerization and conversion: A review of thermochemical methods. *Chemical Engineering & Technology*, 34(1), 29-41.
- Pandey, K. K. (1999). A study of chemical structure of soft and hardwood and wood polymers by FTIR spectroscopy. *Journal of Applied Polymer Science*, 71(12), 1969-1975.
- Qin J., Wolcott M. & Zhang J. (2014a). Use of polycarboxylic acid derived from partially depolymerized lignin as a curing agent for epoxy application. *ACS Sustainable Chemistry & Engineering*, 2, 188-193.
- Qin, J., Liu, H., Zhang, P., Wolcott, M. & Zhang, J. (2014b). Use of eugenol and rosin as feedstocks for biobased epoxy resins and study of curing and performance properties. *Polymer International*, 63, 760-765.
- Shabtai, J.S., Zmierzak, W.W. & Chornet, E. (1999). Process for conversion of lignin to reformulated hydrocarbon gasoline. US Patent 5959167.
- Sun, G., Sun, H., Liu, Y., Zhao, B., Zhu, N. & Hu, K. (2007). Comparative study on the curing kinetics and mechanism of a lignin-based-epoxy/anhydride resin system. *Polymer*, 48 (1), 330-337.
- Thielemans, W. & Wool, R. (2005). Lignin esters for use in unsaturated thermosets: Lignin modification and solubility modeling. *Biomacromolecules*, 6(4), 895-1905.
- Wang, X.Y. & Rinaldi, R. (2012). Solvent effects on the hydrogenolysis of diphenyl ether with Raney Nickel and their implications for the conversion of lignin. *ChemSusChem*, 5(8), 1455-1466.
- Xiao B., Sun X. & Sun R. (2001). The chemical modification of lignins with succinic anhydride in aqueous systems. *Polymer Degradation and Stability*, 71(2), 223-231.
- Xie, Y., Lü, Q., Jin, Y. & Cheng, X. (2011). Enzymatic hydrolysis lignin epoxy resin modified asphalt, *Advanced Materials Research*, 239-242. 3346-3349.
- Xin J., Zhang, P., Wolcott, M., Zhang, X. & Zhang, J. (2014). Partial depolymerization of enzymolysis lignin via mild hydrogenolysis over Raney Nickel. *Bioresource Technology*, 155, 422-426.
- Yan, N., Zhao, C., Dyson, P.J., Wang, C., Liu, L.-t. & Kou, Y. (2008). Selective degradation of wood lignin over noble-metal catalysts in a two-step process. *ChemSusChem*, 1(7), 626-629.

- Yang, D., Qiu, X., Zhou, M. & Lou, H. (2007). Properties of sodium lignosulfonate as dispersant of coal water slurry. *Energy Conversion and Management*, 48, 2433-2438.
- Yang, H., Yan, R., Chen, H., Lee, D. & Zheng, C. (2007). Characteristics of hemicellulose, cellulose and lignin pyrolysis. *Fuel*, 86(12), 1781-1788.
- Yin, Q. & Di, M. (2012). Preparation and mechanical properties of lignin/epoxy resin composites, *Advanced Materials Research*, 482-484, 1959-1962.
- Yu, J., Cong, P. & Wu, S. (2009). Laboratory investigation of the properties of asphalt modified with epoxy resin. *Journal of applied polymer science*, 113 (6), 3557-3563.
- Zhao, C., Kou, Y., Lemonidou, A., Li, X. & Lercher, J. (2010). Hydrodeoxygenation of bio-derived phenols to hydrocarbons using Raney Ni and Nafion/SiO₂ catalysts. *Chemical Communications*, 46(3), 412-414.